TECHNISCHE UNIVERSITÄT DRESDEN

11th German Ferrofluid Workshop

Benediktbeuern
September 28th – 30th
2011

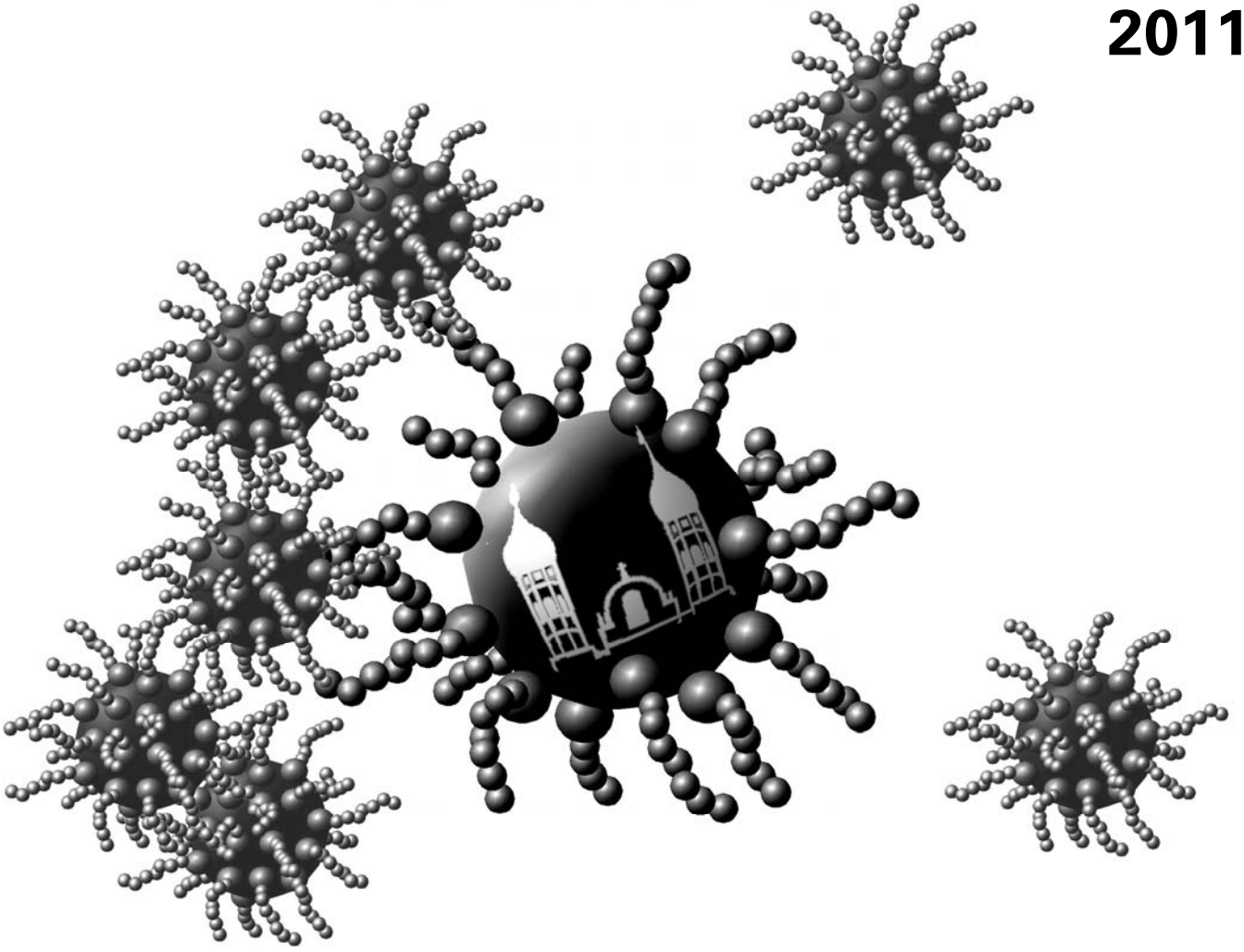

Book of Abstracts

Program of the

11th German Ferrofluid Workshop

Benediktbeuern, 28.9.-30.9.2011

Wednesday, September 28th

14:00 – 14:30	***Opening***		
14:30 - 14:55	Heinrich, D.; Goni, A.R.; Cerioni, L.; Osán, T.; Pusiol, D.J.; Thomsen, C.	*Time dependent NMR spectroscopy on citrate ferrofluids*	22
14:55 - 15:20	Sprenger, L.; Lange, A.; Odenbach, S.	*Thermomagnetic convection in ferrofluids*	54
15:20 - 15:45	Dieckhoff, J.; Ludwig, F.	*Response of spherical magnetic nanoparticles to rotating magnetic fields*	10
15:45 - 16:10	Eberbeck, D.; Müller, R.; Schmidt, C.; Wagner, S.; Löwa, N.; Trahms, L.	*Evidence of bimodal distribution of effective magnetic sizes of magnetic nanoparticles*	16
16:10 - 16:40	***Coffee break***		
16:40 - 17:05	Bender, P.; Tschöpe, A.; Birringer, R.	*Characterization of the local elastic properties of gelatine gels by magnetization measurements using Ni nanorods as probes*	3
17:05 - 17:30	Roeben, E.; Messing, R.; Schmidt, A.M.	*Nanorheology approach using magnetically blocked CoFe2O4 nanoparticles in polymer solutions*	46
17:30 - 17:55	Schrittwieser, S.; Schotter, J.; Schoisengeier, A.; Soulantica, K.; Viau, G.; Lacroix, L.-M.; Lentijo Mozo, S.; Boubekri, R.; Ludwig, F.	*Optically detected hydrodynamic properties of anisotropic magnetic nanoparticles for real time biosensing*	52
17:55 - 18:20	Dutz, S.; Hayden, M.E.; Schaap, A.; Stoeber, B.; Häfeli, U.O.	*Size dependent fractionation of magnetic microspheres for magnetic drug targeting on a microfluidic chip*	14
18:20 - 20:30	***Postersession 1***		

Program of the

11th German Ferrofluid Workshop

Benediktbeuern, 28.9.-30.9.2011

Thursday, September 29th

8:30	***Departure for excursion***		
		Mountain Talk	
	Weeber, R.; Kantorovich, S.; Holm, C.	*Simulation models for ferrogels*	57
17:00	***Return from excursion***		
18:00	***General Assembly of the Ferrofluidverein Deutschland e.V.***		
19:30 - ???	***Conference Dinner***		

Friday, September 30th

9:00 - 9:25	Bähring, F.; Wotschadlo, J.; Voigt, K.; Seyfarth, L.; Fischer, D.; Bergemann, C.; Hochhaus, A.; Clement, J.H.	*Development of a standardized cell-based test system for nanoparticles - evaluating the toxic endpoint*	1
9:25 - 9:50	Marten, G.U.; Gelbrich, T.; Ritter, H.; Schmidt, A.M.	*Hybrid polymeric nanostructures for biomedical applications*	40
9:50 - 10:15	Lyer, S.; Dürr, S.; Mann, J.; Tietze, R.; Schreiber, E.; Alexiou, C.	*Magnetic nanoparticles functionalized with Mitoxantron in cell culture - a real-time cell analysis (RTCA)*	37
10:15 - 10:40	Rahn, H.; Lyer, S.; Eberbeck, D.; Wiekhorst, F.; Trahms, L.; Alexiou, C.; Odenbach, S.	*Semi-quantitative XμCT analysis of nanoparticles content in biological tissue samples after magnetic drug targeting*	44
10:40 - 11:10	***Coffee break***		
11:10 - 11:35	Behrens, S.; Essig, S.	*A "green" process for Co-based magnetic fluids by using room temperature ionic liquids*	2
11:35 - 12:00	Jiang, H.; Dobbrow, C.; Vaidyanathan, M.; Schmidt, A.M.	*Cobalt nanoparticles with tuned pattern formation*	24
12:00 - 12:25	Kavaliou, K.; Polevikov, V.; Tobiska, L.	*Modeling the influence of diffusion of magnetic particles on the stability of magnetic fluid seals*	25

12:25 – 12:45 ***Closing***

Overview of all contributions

Abstracts

for the

11th German Ferrofluid Workshop

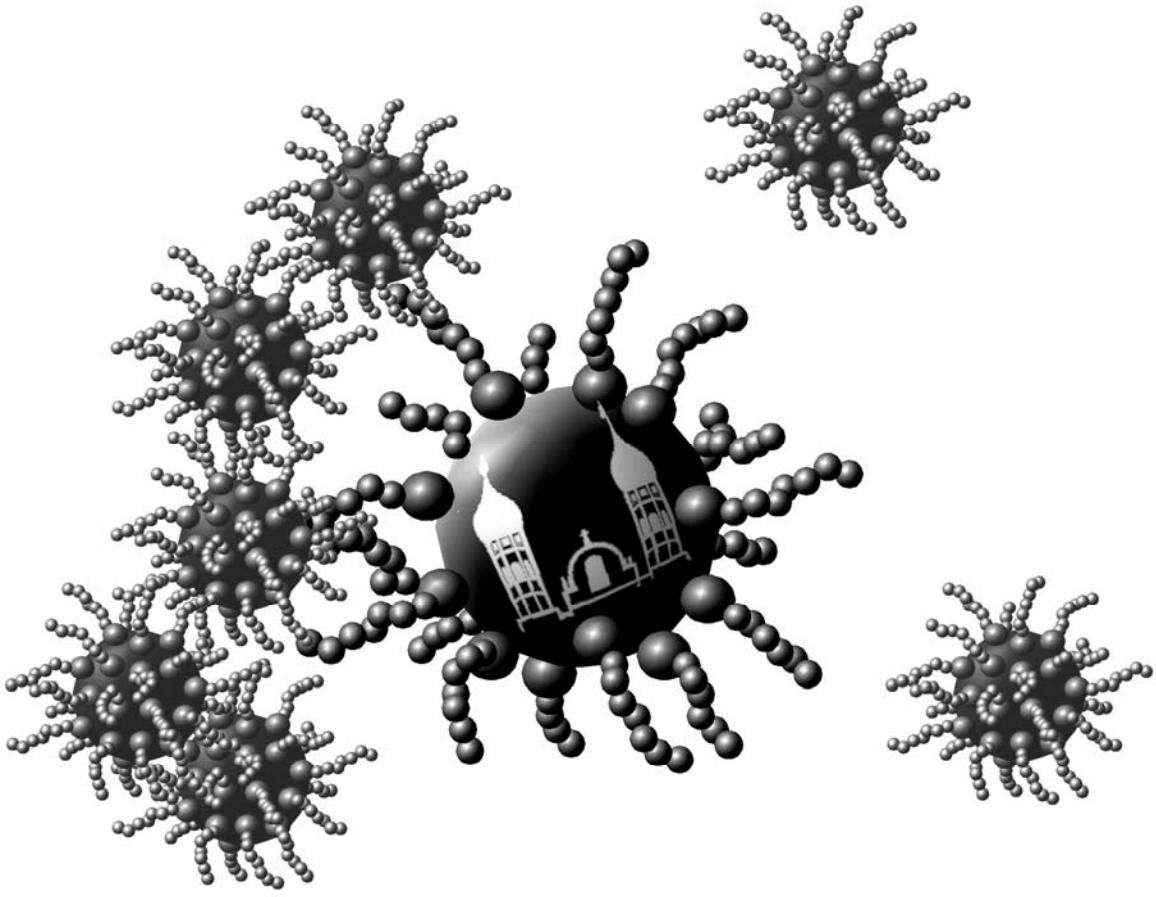

Benediktbeuern, 28.-30.9.2011

DEVELOPMENT OF A STANDARDIZED CELL-BASED TEST SYSTEM FOR NANOPARTICLES - EVALUATING THE TOXIC ENDPOINT

F. Bähring[1], J. Wotschadlo[1,2], K. Voigt[1], Lydia Seyfarth[3], Dagmar Fischer[4], Christian Bergemann[5], Andreas Hochhaus[1], Joachim H. Clement[1]

[1] *Klinik für Innere Medizin II, Abteilung Hämatologie und Internistische Onkologie, Universitätsklinikum Jena, Erlanger Allee 101, D-07747 Jena*
[2] *Institut für Organische Chemie und Makromolekulare Chemie, Friedrich-Schiller-University Jena, Germany*
[3] *Klinik für Frauenheilkunde und Geburtshilfe, Abt. Geburtshilfe, Plazentalabor, Universitätsklinikum Jena, Germany*
[4] *Institut für Pharmazie,Abt. Pharmazeutische Technologie, Friedrich-Schiller-Universität Jena, Germany*
[5] *chemicell GmbH, Eresburgstrasse 22-23, 12103 Berlin, Germany*

Aims: The human brain microvascular endothelial cell line HBMEC is a useful *in vitro* model to study various endothelial cell functions. So far little is known about the interaction of HBMEC and nanoparticles. Microvascular endothelial cells are a key element of the blood-brain barrier. Therefore we asked whether nanoparticles interfere with these cells. In a first step to establish a cell-based model test system for the precise evaluation of nanoparticle-cell interactions we presented data defining the toxic endpoint.

Methods: Positively charged nanoparticles (medium core size 100 nm) with different types of shells (fluidMAG-PEI, fluidMAG-DEAE and fluidMAG-Chitosan) were provided by chemicell GmbH. fluidMAG-D was used as control. HBMEC were seeded in black-walled 96-well culture plates overnight with a density of $1*10^4$ cells per well. After a three hour incubation with various concentrations of nanoparticles three viability assays (CellTiter96® AQ_{ueous} One Solution Cell Proliferation Assay (Promega), MTS-Assay (Promega) and PrestoBlue Cell Viability Assay (Invitrogen)) were tested to determine the number of viable cells. A cytotoxicity assay (CytoTox-ONE, Promega) was used to estimate the number of non-viable cells by the use of the release of LDH from damaged cells. Furthermore the morphology of the cells was analyzed by phalloidin staining and fluorescence microscopy after nanoparticle addition.

Results: Nanoparticle concentrations ranging from 0.5 µg/cm^2 up to 368 µg/cm^2 for all types of nanoparticles each were applied to HBMEC cell cultures. The viability of the cells after incubation with up to 25 µg/cm^2 fluidMAG-PEI nanoparticles was not affected. Higher concentrations caused a dramatic reduction of cell viability. This could be determined with all three cell viability assays (100 µg/cm^2 fluidMAG-PEI: 14-22% viable cells - depending on the assay system used). Furthermore, this could be approved by the LDH assay showing a rising cytotoxicity starting with 50 µg/cm^2 fluidMAG-PEI nanoparticles. In contrast the fluidMAG-DEAE and fluidMAG-Chitosan nanoparticles did not show a significant reduction in cell viability or increase in cytotoxicity even with nanoparticle concentrations up to 368 µg/cm^2. This also holds true with the fluidMAG-D nanoparticles. These data could be further confirmed by documenting the cell morphology during nanoparticle incubation based on the changes of the actin cytoskeleton.

Conclusion: We show that positively charged fluidMAG-PEI nanoparticles are a suitable tool to define the toxic endpoint during the establishment of a standardized test system for nanoparticle-cell interactions.

This work was supported by the Bundesministerium für Bildung und Forschung, 03X0104D

A "Green" Process for Co-based Magnetic Fluids By Using Room Temperature Ionic Liquids

S. Behrens[1], S. Essig[1]

[1] *Institut für Katalyseforschung und –technologie; Karlsruher Institut für Technologie (KIT), Postfach 3640, 76021 Karlsruhe*

Recently, room-temperature ionic liquids (ILs) have attracted great interest, e.g. as reaction medium, reactant or template for the synthesis of inorganic nanomaterials [1]. ILs are well known for their interesting physico-chemical properties, including a low vapour pressure, good thermal stability and high dielectric constants. The properties (e.g., viscosity, polarity, and solvent miscibility) may be tuned by choice of the cation and the anion.

We report a facile and "green" procedure for the synthesis and tailoring of Co-based magnetic fluids by using ILs. ILs provide an excellent medium for the formation and stabilization of nanoparticles, enabling the preparation of nanoparticles without any further stabilizing additives or capping molecules. Non-functionalized ILs provide protective steric/electrostatic layers, which are only loosely bound to the surface of the particles, and thus may readily be displaced by other substances. Hence, the surface properties can easily be engineered according to the specific requirements of the application. Several ILs were investigated for nanoparticle synthesis. The nature of the IL as well as the concentration of the metal precursor influences particle size and size distribution. Figure 1a shows the response of a black-colored Co-MF in octyltrimethylammonium bis-trifluorosulfonylimid to a small magnet.

By adding an appropriate surfactant, the nanoparticles could easily be extracted to form MFs in diverse organic carrier media (e.g., kerosene, L9). Figure 1 shows the phase transfer to kerosene after adding a surfactant (b), mixing (c), and phase separation (d). The remaining clear and colorless IL was again reused for nanoparticle synthesis.

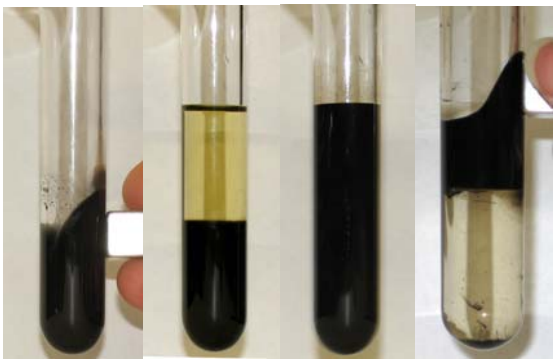

Figure 1. Phase transfer of nanoparticles from an IL-based MF to a kerosene-based MF (lower phase [OMA][BTA], upper phase kerosene)

Furthermore, we synthesized a variety of metal nanoparticles (e.g., Ru, Re, and Ir nanoparticles) by using ILs for nanoparticle stabilization. Such IL-based nanoparticles are interesting for catalytic application.

References

[1] T. Torimoto, T. Tsuda, K. Okazaki and S. Kuwabata, Adv. Mater., 2010, 22, 1196; P. Wasserscheid and T. Welton (Eds.); Ionic Liquids in Synthesis, 2007, VCH-Wiley; J. Dupont and J. Scholten, Chem. Soc. Rev., 2010, 39, 1780.

Characterization of the local elastic properties of gelatine gels by magnetization measurements using Ni nanorods as probes

P. Bender, A. Tschöpe, R. Birringer

Experimentalphysik, Universität des Saarlandes, 66041 Saarbrücken, Germany

1. Introduction

With diameters < 64 nm and aspect ratios > 3 Ni nanorods are uniaxial ferromagnetic single-domain particles [1]. Dispersed in a mechanically soft hydrogel matrix the nanorods rotate in field direction when a homogenous magnetic field is applied, working against the mechanical torque, which is caused by the shear deformation of the gel matrix. When the nanorods are uniaxially aligned it could be shown that the rotation angle of the nanorods can be determined directly by static magnetization measurements [2]. Furthermore, the local shear modulus of the surrounding gel matrix could be estimated.

The present study focuses on the synthesis and characterization of gelatine-based isotropic ferrogels with Ni nanorods as magnetic phase and varying gelatine concentrations. The elastic properties of the ferrogels were extracted from magnetization measurements using a theoretical model, which is based on the Stoner-Wohlfarth-model [3].

2. Synthesis

The nanorods with a mean diameter of ~ 17.4 nm and a mean aspect ratio of ~ 7.2 were synthesized by electro-deposition of Ni into porous alumina templates. The nanorods were released from the templates by dissolution of the alumina layer in aqueous NaOH to which polyvinyl-pyrrolidone was added as surfactant. A thorough washing procedure resulted in stable aqueous colloidal dispersions of the magnetic nanorods. These magnetic fluids were used to prepare gelatine-based ferrogels with four different gelatine concentrations, a hard ferrogel with $10\ \mathrm{wt}\%$ gelatine and three soft ferrogels with $1.5\ \mathrm{wt}\%$, $2\ \mathrm{wt}\%$ and $2.5\ \mathrm{wt}\%$ gelatine.

3. Extended Stoner-Wohlfarth-model

When a SW-particle is dispersed in an elastic environment which allows a significant rotation in field direction the total reduced energy density can be written as follows:

$$\begin{aligned}\epsilon &= \frac{1}{2}sin^2(\Theta - \Phi - fhsin\Phi) \\ &\quad -hcos\Phi + \frac{1}{2}fh^2sin^2\Phi. \qquad (1)\end{aligned}$$

Here, Θ is the angle between the easy axis of the particle and the external field, Φ the angle between the magnetic moment and the external field and f a dimensionless factor depending on both, the geometry (aspect ratio n, magnetic volume V_m, geometrical volume V_g) and magnetism (coercivity H_K, saturation magnetization of Ni M_S) of the nanorods, and on the elastic properties of the matrix (shear modulus G'),

$$f = \frac{3ln(n)}{4n^2}\frac{V_m}{V_g}\frac{\mu_0 H_K M_S}{G'}. \qquad (2)$$

Minimization of Eq. 1 with respect to Φ allows to calculate the hysteresis loops of an isotropic ensemble of SW-particles for a given value of f, from which the dependence of the reduced coercivity $h_C = \mu_0 H_C/\mu_0 H_K$ on f can be extracted (Fig. 1).

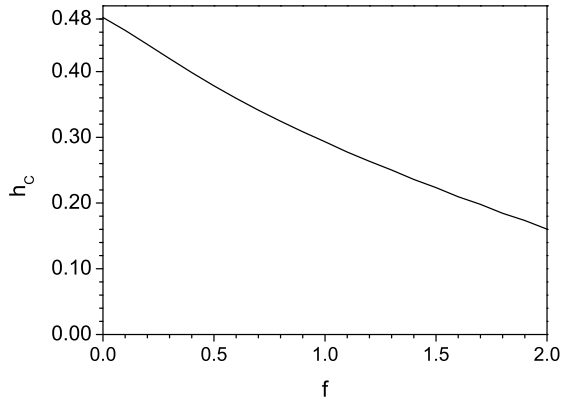

Figure 1: Dependence of the reduced coercivity h_C of an isotropic ensemble of SW-particles on the gel factor f.

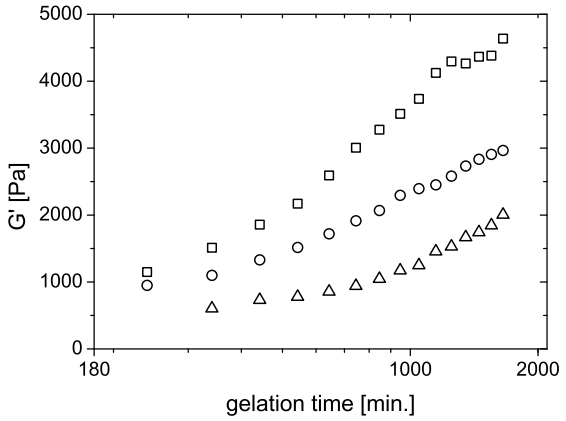

Figure 2: Shear modulus G' of the three soft ferrogels dependent on gelation time (□: 2.5 wt%, ○: 2 wt%, △: 1.5 wt%).

4. Experimental

The objective of this work was to determine the shear modulus of a soft hydrogel matrix using randomly oriented Ni nanorods as probes. Based on the extended SW-model, the analysis proceeded as follows. First, the nanorods were dispersed in a mechanically rigid matrix ($G' \rightarrow \infty \Rightarrow f \rightarrow 0$). Form the measured coercivity of the isotropic ensemble $\mu_0 H_C$, the coercivity of the nanorods $\mu_0 H_K = \mu_0 H_C / 0.48$ could be determined. In the second step, the coercivity of the three isotropic dispersions of nanorods in the soft matrices were measured and normalized to $h_C = \mu_0 H_C / \mu_0 H_K$ and the corresponding gel factor f could be obtained from Fig. 1. Now the shear modulus of the soft gel matrices G' could be calculated using

$$G' = \frac{3ln(n)}{4n^2} \frac{V_m}{V_g} \frac{\mu_0 H_K M_S}{f}. \qquad (3)$$

In particular, the time dependent evolution of G' was monitored.

5. Results

Fig. 2 shows the time dependent shear moduli G' of the three soft ferrogels assuming that $V_m = V_g$. While the absolute values of G' are significantly larger than the macroscopic values, the relative change follows the expected c^2 dependency [4], which implies that such measurements are well-suited for semi-quantitative analysis of the shear modulus after calibration. Furthermore, the estimated shear moduli of the ferrogel with $2.5\ \mathrm{wt}\%$ gelatine are in good agreement with the results in [2].

Acknowledgments
The authors would like to thank Dr. M. Koch for the ESEM-micrographs, as well as Prof. Dr. C. Wagner, C. Schäfer and E. Wagner for the rheometer measurements. Furthermore, the financial support by the Graduiertenförderung of the Universität des Saarlandes is gratefully acknowledged.

References

[1] C.A. Ross et al., Phys. Rev. B 65, 144417 (2002).

[2] P. Bender, A. Günther, A. Tschöpe, and R. Birringer, JMMM 323, 2055 (2011).

[3] E.C. Stoner and E.P. Wohlfarth, IEEE Trans. on Mag. 27, 3475 (1991).

[4] V. Normand, S. Muller, J. Ravey, and A. Parker, Macromolecules 33, 1063 (2000).

Investigation of the phase transition in magnetorheological elastomers using XμCT

T. Borbáth[1], S. Odenbach[2]

[1] *Power Engineering Faculty, University Politehnica of Bucharest, Splaiul Independentei 313, 060042, Bucharest 6, Romania*
[2] *Chair of Magnetofluiddynamics, TU Dresden, 01062, Dresden, Germany*

The phase behavior of polymer solutions and mixtures is a complex issue and is of both technological and fundamental interest.
For a better understanding of the microstructure formation in MREs, X-ray microcomputed tomography (XμCT) investigations were carried out. Three dimensional representations of the magnetic field induced phase separation in dispersions of iron particles are presented. Further, the formation of column structures of magnetic particles in magnetorheological elastomers (MRE) was quantitatively analyzed.

Sample preparation and experimental setup

For the elastomeric matrix the Sylgard 184 elastomer kit from Dow Corning Corporation (USA) was used. This contains a highly transparent silicon elastomer with medium viscosity and a silicone resin solution. The curing agent was added in a mass ratio of 1:10.
As magnetic filler, iron powder with an average particle size of approximately 35 μm was chosen. It has several advantages as being inexpensive, stable and shows a wide range of technological applicability.
The components were dispersed and the polymer blends were cured at a temperature of 90 °C in the presence of magnetic fields. Eight different strengths (220 kA/m, 110 kA/m, 70 kA/m, 55 kA/m, 30 kA/m, 15 kA/m 8 kA/m) were applied in order to investigate phase changes of the structures formed by the dispersed particles in the magnetorheological elastomer samples (see Fig. 1a, b, c).

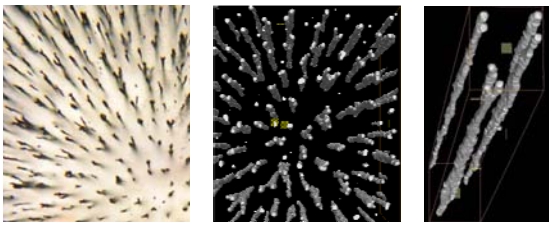

Fig. 1 MRE prepared under H = 220 kA/m: a − picture of the bottom of the sample; b – bottom view of the reconstructed tomography image; c − extracted columns from the reconstructed tomography image.

Each time three samples with 5% mass content of iron powder were prepared, having a diameter of 29 mm and a height of 15 mm.
X-ray tomography experiments were carried out with a laboratory setup, based on a commercial nano-focus tube with transmission target of the product line phoenix/X-ray (GE Measurement and Control Solutions, USA) and a Shad-o-Box 4K detector (Radicon Imaging Corp., USA). Projection images were made with 0.25° angular increment using a tube current of 135 μA and 100 kV as acceleration voltage.
Three dimensional reconstructions were carried out using the VG Studio Max software (Volume Graphics GmbH, Heidelberg, Germany). The reconstructed images were analyzed using the ImageJ 1.44p software.

Results and discussion

The tendency to use quantitative methods instead of qualitative analysis for analyzing the dispersion of different nano- and microstructures is growing recently [1]. An appropriate method for this study is based on Delaunay triangulation offering uniform separation between nearest neighbors [2].
The frequency distribution of the distances between the iron columns given by the Delaunay triangles sides can be well fitted with the normal distribution [3] (see Fig. 2).

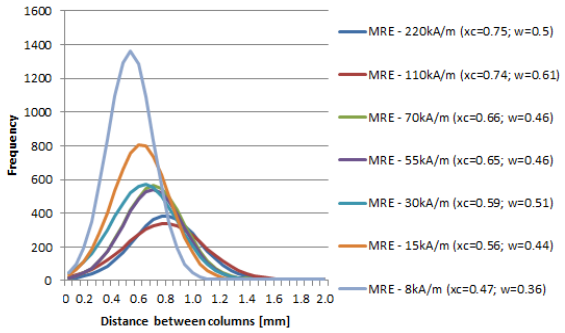

Fig. 2 Gauss fit of column distribution (xc – mean value; w – standard deviation).

With lower magnetic fields the repulsive force between the Fe particles becomes weaker and the number of Fe columns increases (see Fig. 3) while their size decreases (see Fig. 4). Consequently, the peak of the frequency curve is shifted up meanwhile the mean value becomes lower (see Fig. 2).

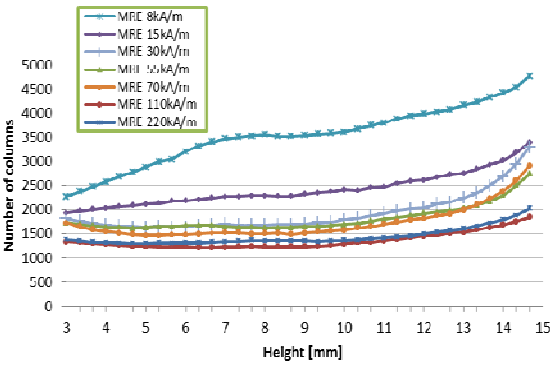

Fig. 3 Vertical distribution of the number of iron columns in different MREs. 3 (15) mm height corresponds to the top (bottom) of the sample.

Bifurcations of the Fe columns are formed close to the bottom of the samples. With lower magnetic fields the bifurcation occurs at greater distances from the bottom (see Fig. 3).

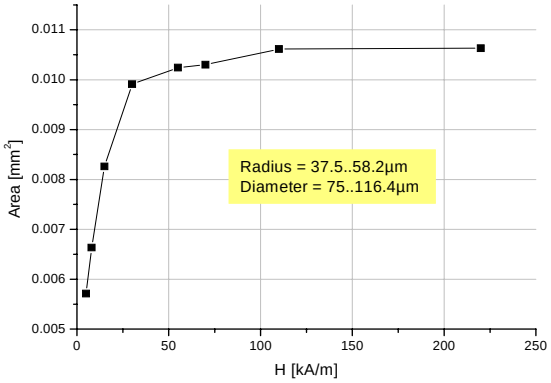

Fig. 4 Average column sizes of MREs prepared under different magnetic field intensities.

Conclusion

It was discovered that it is not necessary to apply very high magnetic fields during the polymerization process of MREs to obtain good column structures. We obtained results for H = 30 kA/m which are similar to those for H = 220 kA/m. From a technological point of view this is an important result.

Outlook

The investigations will be continued by applying even lower magnetic fields during the polymerization process to discover the magnetic field strength from where columns are no longer formed.
The influence of the number and size of the columns on the mechanical and rheological properties of MREs should be investigated, as well.

Acknowledgments

This project is supported by the European Union and the Free State of Saxony.

References

[1] Z. P. Luo, J. H. Koo†, 2007, J. of Microscopy, Vol. 255, pp. 118-125
[2] D. J. Bray, S. G. Gilmour, F. J. Guild, T. H. Hsieh, K. Masania, A. C. Taylor, 2011, J. Mater. Sci., 1573-4803
[3] W. Zhang, X. L. Gong, L. Chen, 2010, J. Magn. Magn. Mater., **322** 3797-801

Dumbbell-like magnetic nanoparticles for the design of asymmetric structures

A. Bushmelev[1], M. Effertz[1], A. M. Schmidt[1*]

[1] *Department Chemie, Institut für Physikalische Chemie, Universität zu Köln, Luxemburger Str. 116, D-50939 Köln*
** E-mail: annette.schmidt@uni-koeln.de*

The combination of ferromagnetic nanoparticles with soft matter, like polymers, surfactants and colloids is attractive with respect to the manipulation, investigation and exploitation of motion on the nanoscale range and for the access to materials with nanoscale anisotropy.
One of our goals is the creation of Janus-like, ferromagnetic nanoparticles with narrow size distribution for the implementation of well-defined nanohybrids. For this purpose, cobalt ferrite ($CoFe_2O_4$) particles are employed, accessible by thermal decomposition of either a mixed oleate [1] or an acetylacetonate [2] complex precursor. A variation of the reaction parameters can be used to result in particles with different size and shape. Since the magnetic nature of the nanoparticles is also size-dependent, tailoring of the properties from superparamagnetic to ferromagnetic is possible. We succeeded in the synthesis of $CoFe_2O_4$ nanoparticles with a diameter between 5 nm and 25 nm, and a narrow size distribution. The particle shape changes with the size from spherical to cubic (Fig. 1).

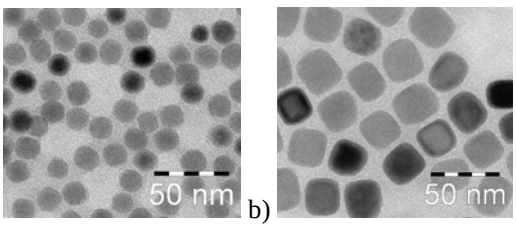

Fig. 1: TEM images of the a) spherical b) cubic $CoFe_2O_4$ nanoparticles

In order to produce nano-objects with amphipatic character, magnetic particles are postfunctionalized. To obtain asymmetric nanoparticles, growing or attaching of noble metal nanoparticles to the surface of primary seed particles is proposed [3,4]. We have managed to optimize the synthesis of so-called dumbbell-like particles with silver and platinum. By varying such parameters as noble metal precursor concentration and cobalt ferrite concentration, it is possible to adjust the size of the attached noble metal particles. It is also possible to produce magnetic particles with multiple noble metal particles attached ("raspberry-like structures", Fig. 2).

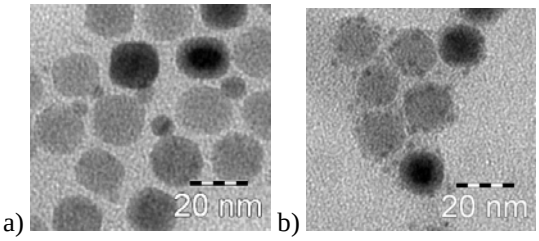

Fig. 2: TEM images of the Ag@$CoFe_2O_4$ particles a) dumbbell-like b) rasp-berry like

The access to ferromagnetic dumbbell-like nano-objects provides great opportunities for the design of materials and surfaces with structural, magnetic or optical anisotropy.

Acknowledgments

We thank Dr. Belkoura, Universität zu Köln for the TEM images. We acknowledge DFG within the framework of NanoSciE+ (ERA) for financial support.

References

[1] N. Bao, L. Shen, *Chem. Mater.*, (21), 3458-3468 **2009**.

[2] S. Sun et al. *J. AM. CHEM. SOC.*, (126), 273-279. **2004**.
[3] S. Sun et al., *Nanoletters.*, Vol. 5, No. 9, 1689-1692 **2005**.
[4] H. Zhang, J. Ding, G. Chow *Langmuir*, (24), 375-378, **2008**.

Magnetic Fluids with Ultra Small Iron Oxide Core/Shell-Particles for Clinical Applications

N. Buske[1] and C. Dunman[2]

[1] *www.magneticfluids.de*
[2] *Capsulution Pharma AG, Volmerstr. 7b, D-12489 Berlin, Germany*

Biocompatible magnetic fluids with optimized magnetic core/shell design are increasingly developed for applications in diagnostics and/or therapy.
Of course, the size of the primary core particles (naked ones) and of the covered particles (core + shell) is different; additionally the particles are normally agglomerated.
The magnetic properties vary with the core size, e.g. using magnetite, MF with super paramagnetic properties (SP) contain sizes up to about 16 nm (measured by TEM images), large single domain particles (LSDP) up to 80 nm show a coercivity and relative magnetization.

The hydrodynamic size of the agglomerated particles measured by dynamic light scattering (DLS, PCS) determines the half live time of blood circulation and colloidal stability. To increase these values, **U**ltra **S**mall **I**ron **O**xide core/shell-agglomerates of 20-30 nm (USPIO) instead of **S**mall **I**ron **O**xide ones of 50-60 nm (SPIO, like RESOVIST®) were more and more used, especially for MRI.

Preliminary results for the preparation /characterization of MF with primary magnetite cores of 5-7 nm with USPIO and SPIO diameters will be described in this paper.
The following stabilizers were used: citric acid, poly aspartic acid, dextran T 9-11. Three different preparation methods were realized:
a) the classical co-precipitation of particles synthesis, the generation of a stabilizer free magnetite SPIO and USPIO-hydrosol as intermediate with consecutively particle modification (two step process),
b) the classical co-precipitation of particles synthesis in presence of the stabilizer (one step-process),
c) the co-precipitation at low Fe-salt concentrations and at high carrier viscosities /1/, within an one step-process.

The advantages/disadvantages of the processes will be discussed in detail.

Stable magnetite MF for in-vivo use with SPIO and USPIO particles could be prepared with a) and b) using dispersion methods (ultra sound) and classification ones (filtering, centrifugation, magnetic separation technique), but with c) USPIO particles were prepared directly without additional fractionation.

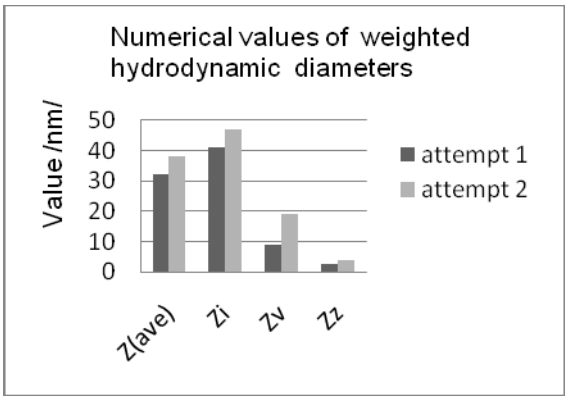

Fig. 1: USPIO-magnetite-MF prepared according to method c), stabilizer: dextran T 9-11.

Acknowledgments
The work was financially supported by the BMBF: NIMINI-MRI Nr. 01EZ0815.

References
[1] E.V. Groman et al.: US patent 6599498

Response of spherical magnetic nanoparticles to rotating magnetic fields

J. Dieckhoff and F. Ludwig

Institut für Elektrische Messtechnik und Grundlagen der Elektrotechnik, TU Braunschweig, Hans-Sommer-Str. 66, 38106 Braunschweig

1. Introduction

The magnetometer based analysis of magnetic nanoparticle (MNP) dynamics, i.e., their response to a time-varying magnetic field has so far been concentrated on ac fields and field pulses, as used in AC susceptibility and magnetorelaxometry (MRX) measurements. These measurement techniques were extensively used for MNPs characterization and allow various biosensor realizations [1].
Another method to study the dynamic properties of magnetic nanoparticles is to analyze their response to a rotating magnetic field. Depending on their characteristic time constant, a phase lag between magnetic field and their magnetic moment will be expected. Based on this effect, Schotter et al. [2] proposed a new homogeneous biosensor.
In this contribution we present a briefly description of a developed measurement setup for MNPs in a rotating magnetic field, first measurement results and a comparison with theory.

2. Experimental setup

To measure the dynamic behavior of the net magnetization of magnetic nanoparticle suspensions, a fluxgate-based system was developed (Figure 1). The used low-noise fluxgates allow one to measure the MNP magnetization stray field, which lies in the nanotesla range. The rotating field generating unit consists of a 2-axes Helmholtz coil and a current control unit based on linear power operational amplifiers. Combined with a data processor providing A/D and D/A converters as well as the measurement software, a rotating magnetic field up to 5 kHz can be supplied. The maximum rotation frequency depends on the field amplitude, which is limited to 10 mT.

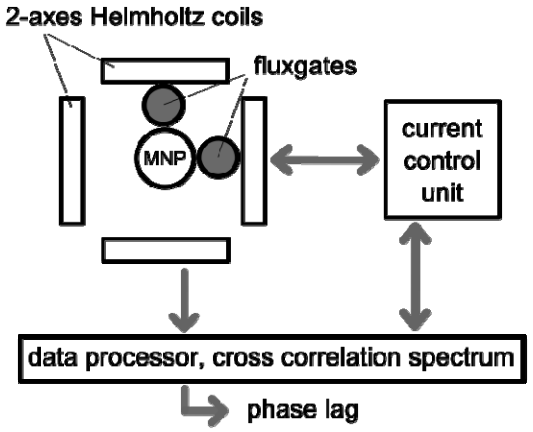

Figure 1. Schematic setup of the measurement system including two fluxgates positioned next to the MNP vessel in the center of the 2-axis Helmholtz coil. Arrows indicate relationships between different system components.

The physical quantity of interest, the phase lag ϕ between the rotating magnetic field and the MNP magnetization, is calculated from the processed fluxgate signals and the Helmholtz coils currents via the cross correlation spectrum.

3. Simulation and measurement results

Assuming that the MNPs are rigid dipoles, Raikher and Shliomis [3] proposed that the nanoparticle dynamics can be described by the following differential equation:

$$\frac{d\vec{M}}{dt} = -\frac{1}{\tau_{par} H_0^2}\vec{H}\left[\left(\vec{M}-\vec{M}_0\right)\vec{H}\right] - \frac{1}{\tau_{perp} H_0^2}\left[\vec{H}\times\left(\vec{M}\times\vec{H}\right)\right]$$

Here H is the rotating magnetic field, M the magnetic nanoparticle magnetization and τ_{perp} and τ_{par} are the time constants perpendicular and parallel to the applied field direction. In the case of a rotating magnetic field with an angular frequency ω, assuming that there is a constant phase lag ϕ and proposing that there is no rotational motion of the carrier medium, one obtains the following solution for the phase lag ϕ and the magnetization amplitude M [4]:

$$\phi = \arctan\left(\omega\tau_{perp}\right) \quad \text{and} \quad M = M_0 \cos\left(\phi\right)$$

First measurements of the phase lag were performed on an aqueous suspension of magnetite (Fe_3O_4) nanoparticles with polymer shells. Details on the nanoparticle parameters can be found in [5]. The measured phase lag spectra (Figure 2) show clearly the predicted arctan behavior as well as a field amplitude dependent spreading. Comparing the results with simulations for monodisperse MNPs, noticeable deviations are observable. However, including a lognormal distribution of the particles core size and hydrodynamic diameter, leads to a much better agreement with the measurement results. The obtained parameters for the mean and standard deviation of the core and hydrodynamic size distribution agree well with those determined with other methods.

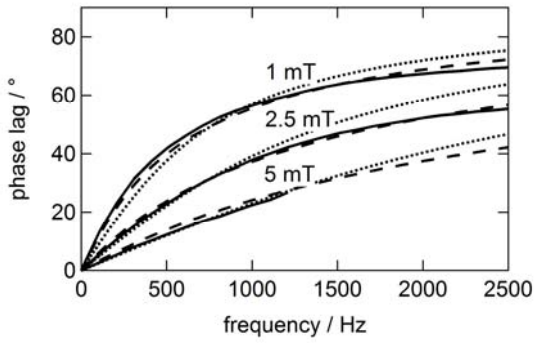

Figure 2. Phase lag spectrum for a rotating filed with 1 mT, 2.5 mT and 5 mT amplitude. Solid lines: measurement results; dotted lines: simulation results for monodisperse nanoparticles with 38 nm core diameter and 95 nm hydrodynamic diameter; dashed lines: simulation results for multidisperse sample with μ_c = 36 nm, σ_c = 0.2, μ_h = 115 nm and σ_h = 0.1.

Acknowledgments

This work was supported by the European Commission FP 7 NAMDIATREAM project (NMP-2010-246479).

References

[1] F. Ludwig, E. Heim, and M. Schilling, J. Magn. Magn. Mater. **321**, 1644 (2009).

[2] S. Schrittwieser, J. Schotter, T. Maier, R. Bruck, P. Muellner, N. Kataeva, K. Soulantika, F. Ludwig, A. Huetten, and H. Brueckl, Procedia Engineering **5**, 1107 (2010).

[3] Y. L. Raikher and M. I. Shliomis, Adv. Chem Phys. 87, 595 (1994).

[4] M. I. Shliomis, in Ferrofluids: Magnetically controllable fluids and their applications, S. Odenbach (Ed.), Springer, 2002 (p. 85).

[5] K. Enpuku, T. Tanaka, T. Matsuda, F. Dang, N. Enomoto, J. Hojo, K. Yoshinaga, F. Ludwig, F. Ghaffari, E. Heim, and M. Schilling, J. Appl. Phys. 102, 054901 (2007).

Immobilization State and Magnetic Behavior of Magnetic Multicore Nanoparticles Injected Into Living Tumors

S. Dutz[1], M. Kettering[2], I. Hilger[2], R. Müller[1], M. Zeisberger[3]

[1] *Department Nano Biophotonics, Institute of Photonic Technology, Jena, Germany*
[2] *Institute of Diagnostic and Interventional Radiology, Jena University Hospital - Friedrich Schiller University Jena, Germany*
[3] *Department of Spectroscopy and Imaging, Institute of Photonic Technology, Jena, Germany*

Magnetic nanoparticles (MNP) are promising tools in modern medicine. One of the main fields of application of them is magnetic heating therapy represented by magnetic particle hyperthermia and thermoablation for the treatment of malign tumors [1]. When exposing a tumor enriched with MNP to an alternating magnetic field, different mechanisms for the reversal of the magnetization of the MNP take place (Neel-relaxation, Brown-relaxation, and hysteresis) which leads to a temperature increase in the tumor and thus damaging of the tumor tissue.

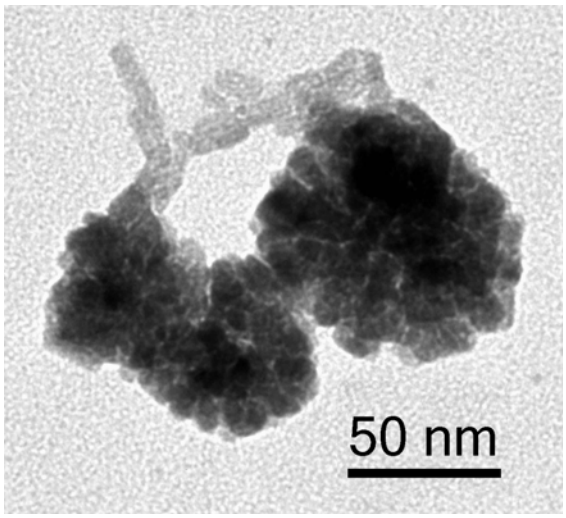

Figure 1: Typical TEM image of the injected multicore nanoparticles.

The proportion of each single reversal mechanism on the heating effect depends on the structural and magnetic properties of the particles and the surrounding medium. The influence of structural and magnetic properties on the specific heating power of the particles is investigated by a lot of groups by in vitro experiments [2]. But for the heat generation inside a living tumor it is of particular interest whether the particles are mobile in the extra- and intracellular liquid or are they fixed to the tumor tissue because these conditions may determine the dominating relaxation mechanism. Up to now the behavior regarding the immobilization state of the MNP in tumor tissue is more or less unknown.

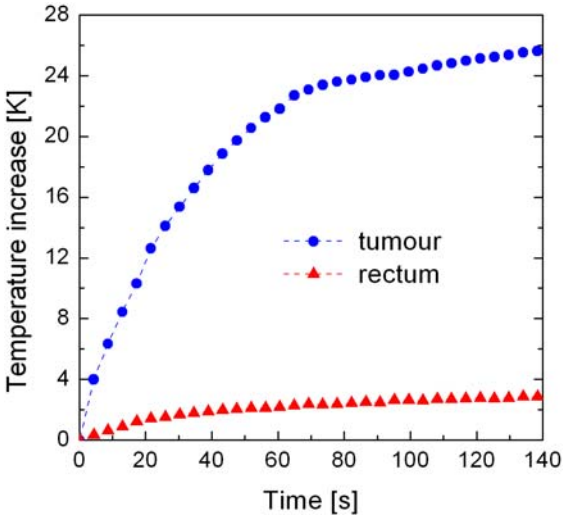

Figure 2: Temperature rise (ΔT) within the tumour (dots) and the rectum (triangle, reference) during magnetic heating treatment of one mouse.

Aim of this contribution was the investigation of this magnetic behavior of MNP injected into tumors in vivo. To this end magnetic multicore particles (Figure 1) prepared as described before [3] were injected into MDA-MB-231 tumors subcutaneously grown between the shoulder blades of female immunodeficient mice. Mice were sacrificed before or after magnetic heating treatment (Figure 2) in an alternating magnetic field (H = 24 kA/m, f = 400 kHz) and tumors were removed for

further investigations. The spatial distribution of the particles inside the tumor was investigated by X-ray images and histological examination. Magnetic properties of the MNP in the tissue were determined by vibrating sample magnetometry and were compared to the properties of the same particles dispersed in water or fixed to a gelatine matrix.

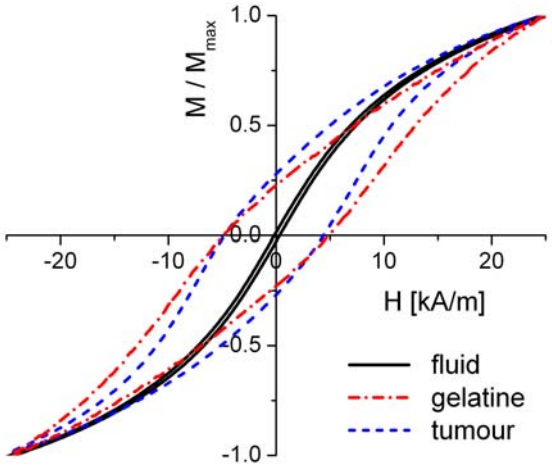

Figure 3: Comparison of the normalized minor loops for mobile MNP in fluid, immobilized MCNP (gelatine), and MCNP inside the tumour at field amplitude of 25 kA/m.

It was found that the injected MNP are relatively inhomogeneously distributed as spots in the tumor tissue. In each spot the spatial distribution of the MNP is predominantly homogeneous without formation of clusters. They show a magnetic behavior like the MNP fixed to a matrix (Figure 3) which means that the MNP are bound relatively tight to the tumor tissue. This is very important for the choice of suitable MNP for magnetic heating therapy. In this case MNP with high hysteresis losses or high Neel-losses (depending on frequency and amplitude of the field) are promising for a successful magnetic heating. In this contribution we show the experimental methods and the results for the investigation of this behavior, describe the performance of magnetic heating treatment on mice, and discuss the importance of our results for further development of MNP for magnetic particle hyperthermia and thermoablation.

Acknowledgments

The authors gratefully acknowledge financial support by the Deutsche Forschungsgemeinschaft (FKZ: ZE825/1-1 and Hi 689/7-1).

References

[1] Hilger I, Andrä W, Hergt R, Hiergeist R, Schubert H, Kaiser WA. Electromagnetic Heating of Breast Tumors in Interventional Radiology: in vitro and in vivo Studies in Human Cadavers and Mice. *Radiology* 218: 570-575 (2001).

[2] Hergt R, Dutz S, Müller R, Zeisberger M. Magnetic particle hyperthermia: nanoparticle magnetism and materials development for cancer therapy. *J. Phys.: Condens. Matter* 18, 2919-34 (2006).

[3] Dutz S, Clement JH, Eberbeck D, Gelbrich Th, Hergt R, Müller R, Wotschadlo J, Zeisberger M. Ferrofluids of Magnetic Multicore Nanoparticles for Biomedical Applications. *J. Magn. Magn. Mater.* 321/10: 1501-1504 (2009).

Size Dependent Fractionation of Magnetic Microspheres for Magnetic Drug Targeting on a Microfluidic Chip

S. Dutz[1,2], M.E. Hayden[3], A. Schaap[4], B. Stoeber[4,5], U.O. Häfeli[1]

[1] *Faculty of Pharmaceutical Sciences, University of British Columbia, Vancouver, Canada*
[2] *Department Nano Biophotonics, Institute of Photonic Technology, Jena, Germany*
[3] *Department of Physics, Simon Fraser University, Burnaby, Canada*
[4] *Department of Mechanical Engineering, University of British Columbia, Vancouver, Canada*
[5] *Department of Electrical and Computer Engineering, University of British Columbia, Vancouver, Canada*

Magnetic microspheres (MMS) typically show a broad size distribution. For clinical magnetic drug targeting, uniform MMS are preferred so that each microsphere responds the same way to externally-applied guiding magnetic field gradients. Furthermore, the MMS must be smaller than red blood cells, but large enough to react to the applied magnetic field gradients. Since the preparation of monodisperse MMS can be challenging, the size-dependent fractionation of MMS with a wide size distribution is a useful tool to obtain MMS with a narrow size distribution.

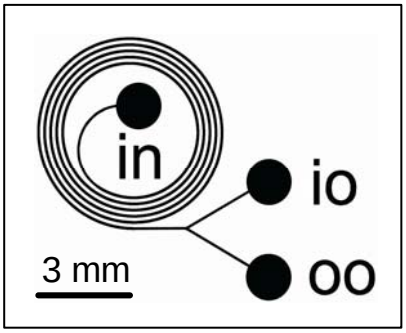

Figure 1: Schematic of the microfluidic MMS fractionation system with inlet (in), outer outlet (oo), and inner outlet (io).

In this contribution we present a microfluidic chip for continuous MMS fractionation based on a combination of shear-induced inertial lift forces that act on particles flowing in a curvilinear channel (i.e., the Dean effect [1-3]) and magnetic forces generated by a magnetic octupole below the chip. The spiral microfluidic structure (Fig. 1) was made using polydimethylsiloxane (PDMS) molding. The chip consists of an inlet (in) at the centre of the spiral, the spiral structure, and a 1:1 flow splitter at the spiral exit, separating the flow into inner and outer streams that can be collected at the inner (io) and outer (oo) outlets. The spiral channel has 5 turns, is 100 µm wide, 60 µm high, and has an outer diameter of about 6 mm. MMS suspensions are driven through the chip by a syringe pump.
Magnetic forces are generated by a magnetic octupole built from 8 axially magnetized rectangular prisms (3 x 3 x 10 mm^3). The magnetic octupole is mounted below the chip and positioned so that the inlet is along the field free axis of the octupole (Fig. 2).

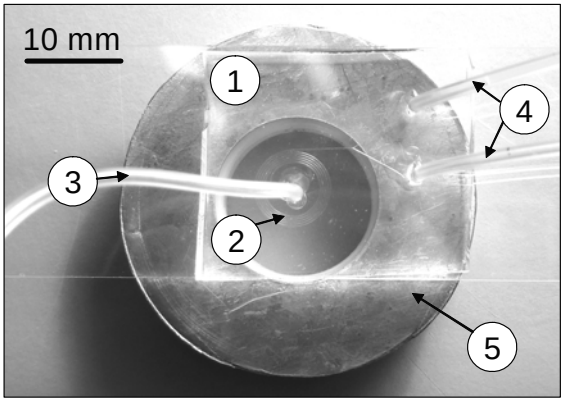

Figure 2: Photograph of the microfluidic chip (1) with spiral structure (2), inlet (3), and outlets (4) above the octupole magnet (5).

The suitability of the chip to separate distinct MMS size populations was confirmed through several experiments. The forces acting on the MMS could be adjusted such that all of the nearly monodisperse (10 µm diameter) particles were found in either the inner stream or the outer stream. In a different test, a mixture of 2 µm- and 12 µm-

diameter particles was separated into its two components. A typical MMS batch with a broad size distribution and a mean diameter of 3.5 µm was also fractionated into samples with mean diameters of 2.8 and 4.3 µm (Fig. 3).

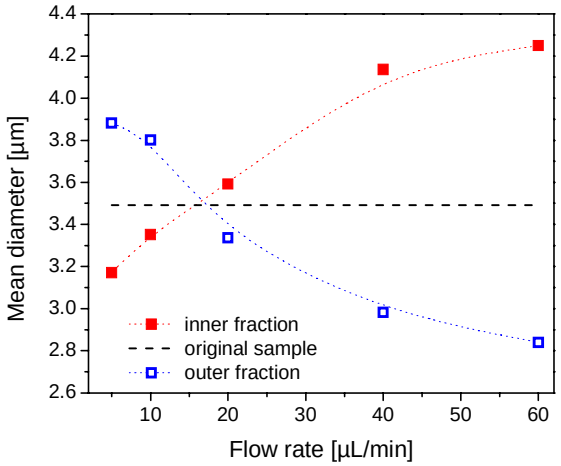

Figure 3: Mean MMS diameter at the outlet ports as a function of flow rate; the input is a polydisperse distribution with mean diameter 3.5 µm.

The chip is thus an appropriate device to concentrate the desired size fractions and to separate particles by size from a polydisperse MMS batch.

Acknowledgments

The authors thank Chemicell, Berlin, Germany and Micromod Partikeltechnologie, Rostock, Germany for MMS samples. The work was funded by a fellowship within the "Postdoc-Programme of the German Academic Exchange Service (DAAD)".

References

[1] Dean WR. Note on the Motion of Fluid in a curved Pipe, *Philos. Mag. Ser.* 7, 208 (1927).

[2] Bhagat AAS et al. Continuous Particle Separation in Spiral Microchannels Using Dean Flows and Differential Migration, *Lab. Chip* 8, 1906 (2008).

[3] Gossett DR and Di Carlo D. Equilibrium Separation and Filtration of Particles Using Differential Inertial Focusing, *Anal. Chem.* 81, 8459 (2009).

Evidence of bimodal distribution of effective magnetic sizes of magnetic nanoparticles

D. Eberbeck[1], R. Müller[2], C. Schmidt[2], S. Wagner[3], N. Löwa[1] and L. Trahms[1]

[1] *Physikalisch-Technische Bundesanstalt, Braunschweig und Berlin, Germany*
[2] *Institut für Photonische Technologien, Jena, Germany*
[3] *Charité, Berlin , Germany*

Introduction

The magnitude of the magnetic moment of a magnetic nanoparticle (MNP) is a crucial parameter for the efficacy of many applications such as e.g. magnetic drug targeting (MDT), hyperthermia MRI and in the new magnetic particle imaging (MPI) method. While for a high MPI signal, (core) sizes of 30...60 nm (single domain magnetite) seem to be appropriate [1], smaller particles show a longer blood half life and extravasate better [2].
Thus, in order to optimise MNP for a given application, the sizes of the different qualities of the MNP, i.e., core, hydrodynamic extension, and effective magnetic domain are of interest. Furthermore, if there is a broad distribution of sizes, different fractions may selectively be targeted (e.g. in MDT larger MNP are attracted by magnet more effectively). Therefore, also the width of the size distribution should be regarded forthepredictionof MNP behaviour.
Here, we compare the size distributions of cores and magnetic moments of different MNP systems and show how bimodality of a size distribution can be identified.

Materials and methods

In the present work we investigated (i) a set of magnetite based single core MNP systems, C1: citrate coated MNP and polymer coated SHP-10, SHP-20 (Ocean NanoTec, USA) and (ii) the commonly used MRI contrast agent Resovist®.
For all size distributions, we assumed spherical particles with diameters d obeying a lognomal function, $f(d)$, and we estimated the diameter of the mean volume, d_V, and the dispersion parameter σ.
The distributions of the core diameters d were estimated by analysing TEM-pictures. Also we obtained the core size *distribution*, in terms of crystallite sizes, analysing the *shape* of the measured intensity distribution of the X-ray diffraction (XRD) intensities $I_m(q)$, measured with a X-ray diffractometer X'Pert Pro MPD. After convolution with the system function, the model

$$I_p(q) = A \int p(L) \left(\frac{\sin(0.5L(q-q_0))}{\sin(0.5a(q-q_0))} \right)^2 \mathrm{d}L \qquad (1)$$

was fitted to $I_m(q)$-data, where A denotes an amplitude factor, a the lattice plane spacing, and q_0 is the center position of the line. Dividing the lognormally distributed cores in parallel columns yields the probability of the length L of columns, p(L).
The distribution $f(d_m)$ of the effective magnetic diameters of (single domain) spheres with the saturation magnetisation M_S was estimated by fitting

$$M(H) = \phi M_S \frac{1}{\overline{V}} \int f(d_m) \frac{\pi}{6} d_m^3 L \, \mathrm{d}d + M_p \qquad (2)$$

to the $M(H)$-data, measured using a commercial susceptometer (MPMS, Quantum Design). ϕ, M_S and $\overline{V}$ are the volume fraction of magnetite, saturation magnetisation and mean volume of MNP, respectively. Here, we had to add a magnetisation M_p which allows for weakly magnetic structures which are evident by the absence of a typical saturation behaviour (fig. 1). Because the origin of M_P is still unknown, (it is not a simple paramagnetic signal), we have approximated M_p phenomenological by $M_p = A_p L(d_p)$, with amplitude A_P and a relative small diameter d_P.
By magnetorelaxometry (MRX) we measured the relaxation of the magnetisation of immobilised MNPs after a polarising field was switched off. Fitting the Moment Superposition Model (MSM) to magnetic re-

laxation decays is another way to obtain $f(d_m)$[3].

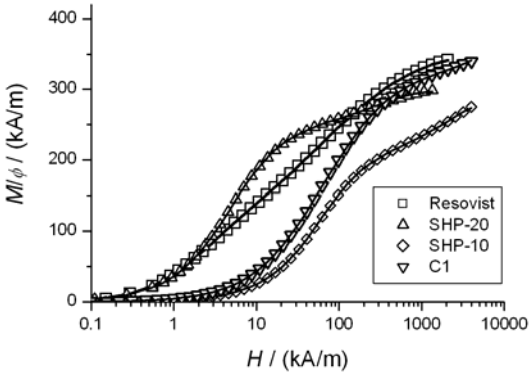

Figure 1: Magnetisation curves of indicated MNP samples together with best fit lines of (2).

Results and discussion

The core size distribution parameters estimated by TEM and by XRD agrees well for the single core systems C1, SHP-10 and SHP-20, being (XRD) d_V=5.4(3) nm, 9.5(2) nm, 17(5) nm and σ=0.37(2), 0.10(3), 0.15(1), respectively. Furthermore, the magnetic size distributions of these systems, derived from $M(H)$-data, $d_{V,m}$=7.1(2) nm, 9.5(3) nm, 20(1) nm and σ=0.31(1), 0.11(1), 0.16(3), respectively, are close to that of the core size distributions. For SHP-20, this is supported by MRX-result, $d_{V,m}$ = 17(2)nm. Note that the relaxation signal of the small MNP of C1 and SHP-10 is below our measurement time window.

Resovist having a mean diameter of single cores of 5 nm (TEM on non-aggregated MNP, fig. 3), exhibits a much shallower magnetisation curve, which indicates a d_m-distribution that is much broader than the TEM data predict. Furthermore, the observation of a strong MRX-signal indicates the presence of 13 nm MNP, also not compatible with the TEM-data.

These confusing observations can be explained by introducing a bimodal size distribution in eq. (3), $f = (1-\beta_2) f_1 + \beta_2 f_2$ with volume fraction β_2. As the result, the small fraction f_1 in Resovist can be identified with the single core fraction, while f_2 with β=30%, is attributed to clusters. The presence of larger structures is also supported by DLS and SAXS-data [4, 5]. This correlates well with the MRX results, if only the β_2=30% of f_2 (f_1 do not make a MRX signal) is considered within the model (fig. 3).

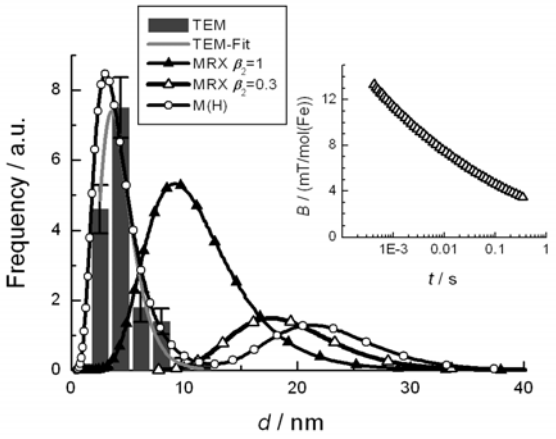

Figure 3: Distribution of core and effective magnetic diameters obtained by indicated method for Resovist. The inset shows the MRX-data.

In conclusion, we showed that for single core MNP the core size distribution equals the magnetic one, while for Resovist a second magnetic size fraction (clusters) was put in evidence, explaining the observed relatively high MPI performance of Resovist. Furthermore, the magnetisation data, $M(H)$, deliver information about the presence of weak magnetic MNP constituents which has to be modelled if magnetic size distribution will be extracted from these data.

Acknowledgements

The research was supported by the German Ministry for Education and Research (FKZ 13N11092), and by the German Research Foundation (KFO 213).

References

[1] A. K. Gupta and M. Gupta, Biomaterials 26, 18 (2005), 3995-4021.
[2] B. Gleich, WO2004/091398 A2 (28.10.2004).
[3] D. Eberbeck, F. Wiekhorst, U. Steinhoff, L. Trahms, J. Phys.: Condens. matter 18 (2006), S2829-S2846
[4] D. Eberbeck, C. Bergemann, F. Wiekhorst and G. Glöckl, Magnetohydrodynamics **41**, 305 (2005).
[5] A. F. Thünemann, S. Rolf, P. Knappe, and S. Weidner, Anal. Chem. **81**, 296 (2009).

Experimental investigations on a branched tube model in magnetic drug targeting

K. Gitter, S. Odenbach

Technische Universität Dresden, Chair of Magnetofluiddynamics, 01062, Dresden, Germany

1. MDT as tumour treatment

Magnetic drug targeting, because of its high targeting efficiency, is a promising approach for tumour treatment. Unwanted side effects are considerably reduced, since the nanoparticles are concentrated within the target region due to the influence of a magnetic field. While in vivo investigations are promising [1, 2], and precise measurement methods have been developed [3], the understanding of hydrodynamics and transport phenomena [4-8] is still a challenge, both with regard to targeting the particles towards the chosen region, as well as capturing them in the target area. This work presents experimental results for a branched tube model. Quantitative results describe e.g. the net amount of nanoparticles that are targeted towards the chosen region due to the influence of a magnetic field. Novel drug targeting maps, combining e.g. the magnetic volume force, the position of the magnet and the net amount of targeted nanoparticles are presented. The targeting maps are valuable for evaluation of setups.

2. Experimental setup and artery-model

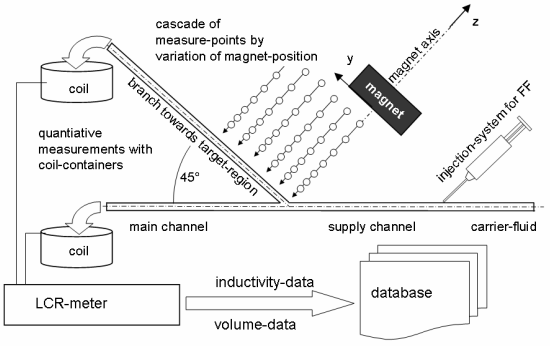

Fig 1: Setup with artery-model and cascade of magnet-positions as points of measurement

Fig. 1 shows the setup around the artery-model and the cascade of chosen positions of the permanent magnet. For each position of the magnet an injection-procedure is performed: In 10 minutes 1ml of ferrofluid is injected into the supplying tube to the flow of distilled water modelling the blood flow. For drug targeting, the use of a ferrofluid must comply with medical restrictions regarding biocompatibility. A water-based ferrofluid of Ferrotech® with magnetite particles is chosen to allow model experiments to conform with physical parameters close to those restrictions. Distilled water is was chosen as the carrier fluid to allow the use of water-based ferrofluids. In choosing the model and the ferrofluid, the parameters required by medical application were approached as closely as possible so that the results may be applied to future medical investigations.

3. Quantitative data

Quantitative data is obtained by measuring the inductivity of calibrated coil-containers capturing the outflow of each branch. The diluted ferrofluid in the coil has a certain permeability that depends on the ferrofluid concentration in the mixture. The resulting change in the coil's inductivity, measured with an LCR meter, allows quantification of the ferrofluid concentration in the containers. The coils are calibrated by variation of the total fluid volumes and ferrofluid concentrations.

4. Quantitative targeting maps

As a result of measurements, novel drug targeting maps, combining e.g. the magnetic volume force, the position of the magnet and the net amount of targeted nanoparticles are presented in [9,10]. In a first targeting-map [9], which summarizes results for 63 magnet posistions, the concentration of the injected ferrofluid is 2.95vol%. Up to 97% of the nanoparticles were successfully targeted into the chosen branch; however, the region where yield was considerable is rather small. A high concentration of injected ferrofluid brings the danger of accretion in the tube. It is shown that an increase in magnetic volume force does not necessarily lead to a higher amount of targeted nanoparticles.
In a second targeting-map [10] the concentration of injected ferrofluid is reduced to 0.14vol%. At a first glance the result with low concentration is promising, since the danger of accretion is avoided.
Nevertheless, one has to consider, that, unless the magnetic volume force in the branch-point was provided in the necessary strength, an application would not be successful.

5. Focus on variation of concentration

The current focus of the investigations is the variation of the concentration of the injected ferrofluid. The range of concentration is between 2.95vol% of the first map and 0.14vol% of the second map. One series of measurements of constant concentration comprises the variation of the magnet-positions where the axis of the magnet points directly towards the branch-point. Systematic measurements will give further insight to the flow phenomena and will provide information how to choose concentrations of future targeting maps.

Acknowledgments

The financial support by Deutsche Forschungsgesellschaft DFG-OD18-13 is gratefully acknowledged.

References

[1] C. Alexiou, R. Jurgons, R. Schmidt et al, “In vitro and in vivo investigations of targeted chemotherapy with magnetic nanoparticles,” J. Mag. Mag. Mat. **293**, 389-93 (2005).

[2] C. Alexiou, R. Jurgons, R. Schmidt, and C. Bergemann, In: *Magnetically controllable fluids and their applications*, ed.: S. Odenbach, (Springer, Heidelberg, New York, 2002).

[3] H. Rahn, I. Gomez-Morilla, R. Jurgons et al, “Tomographic examination of magnetic nanoparticles used as drug carriers,” J. Mag. Mag. Mat. **10**, 321 (2009).

[4] R. Ganguly, B. Zellmer, and I. K. Puri, “Field-induced self-assembled ferrofluid aggregation in pulsatile flow,” Physics of Fluids **17,** (2005).

[5] E. J. Furlani and E. P. Furlani, “A model for predicting magnetic targeting of multifunctional particles in the microvasculature,” J. Mag. Mag. Mat. **312**, 187 (2007).

[6] R. M. Erb, D. Sebba, A. A. Lazarides et. al, “Magnetic field induced concentration gradients in magnetic nanoparticle suspensions: Theory and experiment,” J. Appl. Phys**. 103**, 063916 (2008).

[7] A. D. Grief and G. Richardson, “Mathematical modelling of magnetically targeted drug delivery,” J. Mag. Mag. Mat. **293**, 455-63 (2005).

[8] P.A. Voltairas, D.I. Fotiadis, and L.K. Michalis, “Hydrodynamics of magnetic drug targeting,” J. Biomechanics **35,** 813-21 (2002).

[9] K. Gitter and S. Odenbach,“ Quantitative targeting maps based on experimental investigations for a branched tube model in magnetic drug targeting,” J. Mag. Mag. Mat. doi:10.1016/j.jmmm. 2011.06.055.

[10] K. Gitter and S. Odenbach,“Experimental investigations on a branched tube model in magnetic drug targeting,” J. Mag. Mag. Mat. **323**, 10 (2011).

Siloxane-Functionalized Cobalt Nanoparticles: Syntheses, Characterization, and Catalytic Application

A. Gorschinski[1], W. Habicht[1], O. Walter[2], E. Dinjus[1], S. Behrens[1]

[1] *Institut für Katalyseforschung und –technologie; Karlsruher Institut für Technologie (KIT), Postfach 3640, 76021 Karlsruhe*
[2] *European Commission, Joint Research Centre, Institute for Transuranium Elements, Hermann-von-Helmholtz-Platz 1,76344 Eggenstein-Leopoldshafen*

Functional magnetic nanoparticles have recently attracted increasing interest in catalysis research. Silica-encapsulated nanomagnets, e.g., have been used for the immobilization of homogeneous and heterogeneous catalysts. Such multifunctional magnetic catalysts reveal sustainable catalytic activities and great advantages for catalyst recycling processes.
As previously reported, superparamagnetic metal nanoparticles (e.g., Co and Fe nanoparticles) were synthesized by thermal decomposition of the corresponding metal carbonyls (viz. $Co_2(CO)_8$ or $Fe(CO)_5$) in the presence of amino-functionalized siloxanes, yielding stable metal nanoparticles with free siloxane functionalities [1]. Though, the Co nanoparticles with short-chained aminoalkyl siloxanes (e.g., 3-aminopropyl triethoxysilane (APTES), 4-aminobutyl triethoxysilane) initially assembled into mesoscale spherical particles (up to 0.8 µm), maintaining the superparamagnetic character of the individual nanoparticles. In this case, the individual nanoparticles could only be stabilized colloidally by adding further surfactants.

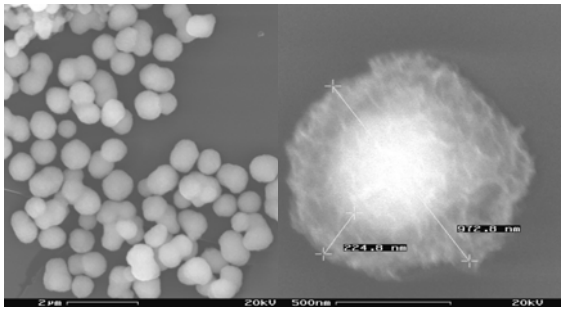

Figure 1: Spherical assemblies of Co@APTES nanoparticles (left) before and (right) after SiO_2 coating.

Therefore, we investigated the synthesis of Co nanoparticles in the presence of various alternative siloxanes with long aminoalkyl chain. With these siloxanes, we prepared individual Co nanoparticles without forming aggregates (Figure 2), a prerequisite for preparation of magnetic fluids.

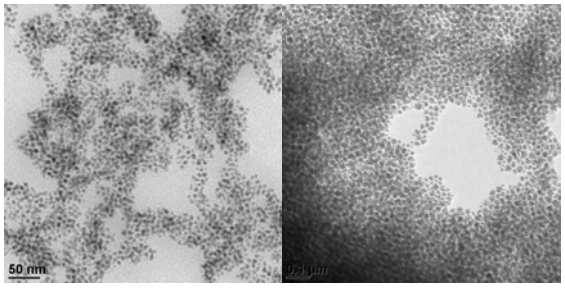

Figure 2: Co nanoparticles functionalized with long-chain aminosiloxanes: (left) Co@TMSPDA, (right) Co@AUDTES.

Size, crystal structure, and magnetic properties of the particles were characterized by TEM/EFTEM, REM/EDX, DLS, XRD, AES-ICP, and magnetic measurements.
The siloxane-functionalized particles were further coated by a SiO_2 layer and used for immobilization of homogeneous and heterogeneous catalysts (Figure 1). The hydroformylation of 1-octene, e.g., has been tested as a model reaction. The activity, selectivity, and magnetic recycling of an immobilized rhodium catalyst were investigated and will be addressed.

References

[1] A. Gorschinski, G. Khelashvili, D. Schild, W. Habicht, R. Brand, M. Ghafari, H. Bönnemann, E. Dinjus, S. Behrens, J. Mater. Chem., 2009, 19, 8829.

Yield stress in ferrofluid influenced by the geometrical parameters of the shear cell

Th. Gundermann, D. Borin, S. Odenbach

Technische Universität Dresden, Chair of Magnetofluiddynamics, 01062, Dresden, Germany

Rheological measurements of various suspensions are often influenced by geometrical boundary conditions of the shear cell. In the current work the influence of the surface roughness on the yield stress in ferrofluids with different composition has been studied.

For the current study we used a fluid based on spherical magnetite nanoparticles (FF-1) prepared by N. Mattoussevitch (Strem Chemicals GmbH) with kerosene as carrier liquid and a fluid with Ba-ferrite nanoplatelets (FF-2) prepared by R. Müller (IPHT, Jena) with a vacuum oil - Pfeiffer P3 - as carrier liquid. In the experiments a shear stress controlled rheometer utilizing a plate-plate geometry made of aluminum with surface roughness Ra=0.08 μm (set 1 - smooth) and Ra=9.41 μm (set 2 - rough) has been used.

In figures 1 and 2 the yield stress τ_y measured for different surface roughness for both samples is presented for varying gap size *h*. The yield stress for the rough surfaces is larger for the same field strengths than compared to the smooth surface. This is in agreement with the result obtained for magnetorheological fluids [2] and can be explained with an induced wall-slip effect for the smooth surface. Nonetheless there are two distinct differences for the different fluids concerning the gap size dependence of the yield stress. The yield stress of the fluid FF-1 increases for small values of the gap, reaches a maximum and than decreases approaching zero. This trend has been observed for both sets, although the maximum for the smooth surface is shifted to larger gap size values. For the sample FF-2 an increase of the gap between the plates results in a decrease of the yield stress for both sets.

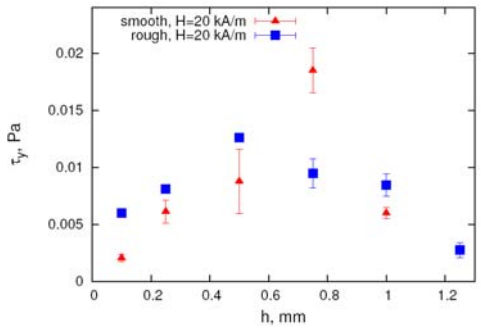

Figure 1. Yield stress of the sample FF-1 as a function of the gap size for H=20 kA/m.

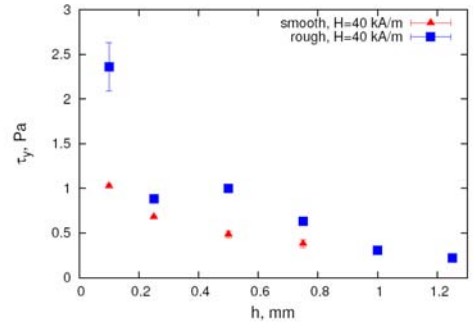

Figure 2. Yield stress of the sample FF-2 as a function of the gap size for H=40 kA/m.

From a theoretical point of view [2] a larger gap between the plates results in a reduced stability of the structures and in a decreasing yield stress. This trend is observed for the fluid FF-2 for the whole range of gap sizes. The increase of the yield stress in the range of small gap size in fluid FF-1 can be qualitatively explained with the wall-sleep effect, however a quantitative estimation of this trend is possible for gap sizes in the range of several nanometers only. Thus, further experiments and theoretical approaches are needed to explain the observed effects.

[1] E. Lemaire and G. Bossis J. Phys. D: Appl. Phys. 24 (1991) 1473-1477.

[2] A. Zubarev and L. Iskakova Physica A 365 (2006) 265-281.

Time dependent NMR spectroscopy on citrate ferrofluids

D. Heinrich[1], A.R. Goñi[2], L. Cerioni[4], T. Osán[3,4], D.J. Pusiol[3,4], C. Thomsen[1]

[1] *Institut für Festkörperphysik, Technische Universität Berlin, Hardenbergstraße 36, 10623Berlin, Germany*
[2] *ICREA, Institut de Ciència de Materials de Barcelona, Esfera UAB, 08193 Bellaterra, Spain*
[3] *Facultad de Matemática, Astronomía y Física, Medina Allende s/n, Ciudad Universitaria, Córdoba X5016LAE, Argentina*
[4] *SPINLOCK S.R.L., Avenida Sabattini 5337, Ferreyra, Córdoba X5016LAE, Argentina*

Magnetic nanoparticles colloidally suspended in a ferrofluid exhibit a tendency to form clusters and chain-like structures under the influence of an external magnetic field; an effect which in the past years has been extensively studied theoretically [1-3] as well as experimentally [4-7]. Recently we used Raman and NMR spectroscopy to monitor the metastable cluster formation and its dynamics in surfacted and ionic ferrofluids [5-7].

In this work, we present results of a study of the magnetic-field induced behavior of a water-based citrate ferrofluid (CFF) with a concentration of 1 vol% using nuclear magnetic resonance (NMR) spectroscopy. A low-resolution NMR spectrometer working at room temperature with a homogenous magnetic field of 225 mT was used for the NMR measurements. The CFF sample was also subjected to a strongly inhomogeneous magnetic field of about B_{inh} = 200 mT generated by an external permanent magnet for different dwell times τ_{inh} from 10 s to several minutes in order to investigate the effect of magnetophoresis on the particle aggregation and clustering dynamics.

Here we make explicit use of the ability of nuclear magnetic resonance (NMR) to distinguish between different magnetic environments of water protons [8] in order to monitor in real time the clustering processes of the magnetic nanoparticles of a water-based citrate ferrofluid (CFF) immersed in the homogeneous field of the NMR spectrometer. Fig. 1 shows two NMR spectra of the CCF sample at the beginning and the end of a measurement series, where the NMR signal was monitored continuously by acquiring a spectrum subsequently every 10 s for more than 10.000 s. Frequencies are measured relative to the Larmor frequency of protons in pure water in the NMR field of 225 mT. Different features are attributed to the different environments experienced by protons in the ferrofluid. The frequency shift and line broadening are signature of strongly inhomogeneous magnetic field and gradient distributions, respectively, produced by the magnetic grains of the ferrofluid and sensed by the protons during their restricted diffusion in the time scale of the NMR experiment (1 ms) [8]. The main peak with the large shift of about 74 kHz is associated to water protons within layers near and around the magnetic poles of the nanograins (i.e., strong field regions). For the whole duration of the NMR-measurement sequence we observe no appreciable change of its frequency; only a phase flip by π is detected.

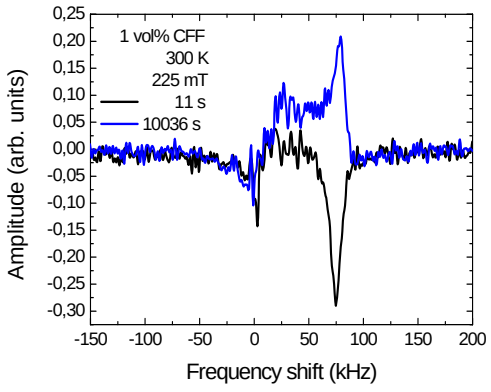

Fig. 1 Two NMR spectra of the CFF sample at the beginning (black) and the end (blue) of a measurement sequence.

In Figs. 2a and 2b, the amplitude and position of the most prominent peak in each spectrum of the IFF and CFF samples, re-

spectively, are plotted for comparison as a function of time. Whereas the peak of the IFF shifted to lower frequencies from 17 kHz to 3 kHz, the peak of the CFF remains at very high values between 75 and 80 kHz. The monotonous decrease with time of the amplitude of the main NMR peaks that sets in at around 400 s and 3000 s for the IFF and CFF, respectively, we infer that the magnetic grains aggregate to field-aligned chains [7]. For the IFF, though, the appearance of the low frequency peak and its strongly increase in amplitude with time were taken as signature of the formation of zipped-chain pseudo-crystalline superstructures [7]. In clear contrast, there is no evidence of the building of such superstructures for the citrate ferrofluid, at least if placed in a homogeneous magnetic field.

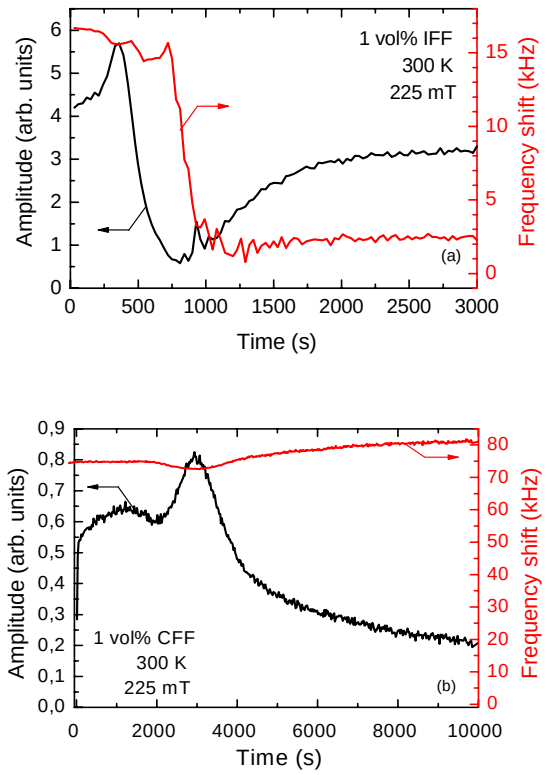

Fig.2 Dependence on time of the amplitude and position obtained by fitting the line shape function to the main peak of each NMR spectrum of (a) the IFF (b) the CFF series.

The situation drastically changes, if the CFF sample is placed in an inhomogeneous field of about 200 mT. Figure 3 shows two NMR spectra of the CFF after been subjected to the inhomogeneous field for different dwell times τ_{inh}. After 90 s in the inhomogeneous field, magnetophoresis has effectively triggered superstructure formation. The evidence for that is the very strong peak apparent in the NMR spectra of the CFF centered at about 3 kHz, exhibiting a similar time evolution of its amplitude as for the case of the IFF sample. The main reason for the different behavior exhibited by both ferrofluids in their clustering dynamics may arise from the fact that the average particle size in the CFF is ten times smaller than for the IFF.

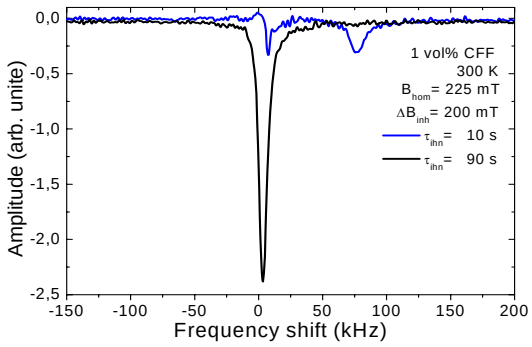

Fig. 3 NMR spectra of the citrate ferrofluid at different times in an inhomogeneous field of 200 mT.

Acknowledgments

Special thanks are due to N. Buske from Magnetic Fluids for producing and providing the ferrofluid samples.

References

[1] A.O. Ivanov, Z. Wang, and C. Holm, Phys. Rev. E **69**, 031206 (2004).

[2] H. Morimoto, T. Maekawa, and Y. Matsumoto, Phys. Rev. E **68**, 061505 (2003).

[3] Z. Wang, C. Holm, and H.W. Müller, Phys. Rev. E **66**, 021405 (2002).

[4] A. Wiedenmann, J. Magn. Magn. Mat. **272-276**, 1487 (2004).

[5] J.E. Weber, A.R. Goñi, D.J. Pusiol, and C. Thomsen, Phys. Rev. E **66**, 021407 (2002).

[6] D. Heinrich, A.R. Goñi, and C. Thomsen, J. Chem. Phys. **126**, 124701 (2007).

[7] D. Heinrich, A. R. Goñi , A. Smessaert, S. H. L. Klapp, L.M. C. Cerioni, T. M. Osán , D. J. Pusiol, and C. Thomsen, PRL **106**, 208301 (2011)

[8] C. E. González, D. J. Pusiol, A. M. Figueiredo Neto, M. Ramia, and A. Bee, J. Chem. Phys. **109**, 4670 (1998).

Cobalt Nanoparticles with Tuned Pattern Formation

H. Jiang[1], C. Dobbrow[2], M. Vaidyanathan[3], A. Schmidt[1*]

[1] *Department Chemie, Institut für Physikalische Chemie, Universität zu Köln, Luxemburger Str. 116, D-50939 Köln, *E-mail: Annette.Schmidt@uni-koeln.de*
[2] *Celin Dobbrow, Mercedes Benz Werk Düsseldorf, Rather Str. 51, 40476 Düsseldorf*
[3] *National Institute of Technology, Dumas Road, Ichchhanath Surat-395007, India*

The study of ferromagnetic single domain nanoparticles made from iron, cobalt and nickel belongs to an active field of basic research. These nanoparticles show a variety of unusual properties and form different nanostructures such as rings and chains under specific environment, which can often be attributed to the anisotropic and strong dipolar interaction between the nanoparticles.

However, highly magnetic nanoparticles such as iron or cobalt suffer greatly from the low stability against oxidation. Various reports show that highly monodispersed cobalt particles can be produced by the hot injection method[1] in the presence of a suitable surfactant. Recently we synthesized a series of polystyrene-coated cobalt nanoparticles using carboxylic acid-telechelic polystyrene as surfactant by a modified procedure of Pyun et al.[2] The obtained nanoparticles show good oxidation resistance and especially different magnetic properties which can be directly influenced by the amount of trioctylphosphineoxid (TOPO) added to the reaction.

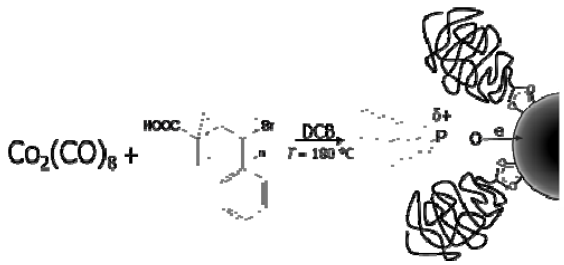

Fig 1. Synthesis of cobalt nanoparticles coated with polystyrene in a one step reaction.

These cobalt nanoparticles were characterized by TEM, vibrating sample magnetometry (VSM), dynamic light scattering and AC susceptometry.

The cobalt nanoparticles synthesized at varying TOPO concentration show an interesting trend in their tendence to form chains of particles, as observed in TEM and cryo-TEM.
The interesting superstructures can be further tuned by an external magnetic field, revealing an equilibrium and transformation among single nanoparticles, rings and chains (see Fig 2).

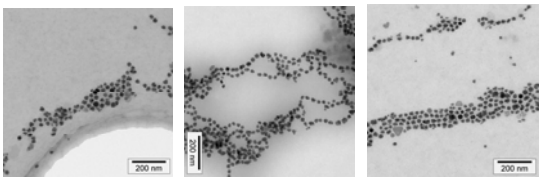

(a) (b) (c)

Fig 2. TEM image taken under different strength of magnetic field of cobalt nanoparticles prepared with 12.7 mmol/L of TOPO: (a) 0 mT, (b) 2 mT, (c) 25 mT.

Acknowledgments

We gratefully acknowledge Dr. Belkoura for TEM images, and DFG and DAAD (WISE program) for financial support.

References

[1] Gürler, C.; Feyen, M.; Behrens, S.; Matoussevitch, N.; Schmidt, A. M., *Polymer* **2008,** *49* (9), 2211-2216.
[2] Korth B., Keng P, Shim I., Bowles S., Tang C., Kowalewski T., Nebesny K., Pyun J., *JACS* **2006**, *128*, 6562-6563

Modeling the influence of diffusion of magnetic particles on the stability of magnetic fluid seal

K. Kavaliou and L. Tobiska

Institut für Analysis und Numerik, Otto-von-Guericke-Universität Magdeburg, Postfach 4120, D-39106 Magdeburg

Introduction

We derive a mathematical model for studying the stability of dynamic magnetic fluid seal under the action of external pressure drop. First results have been published for a simplified version of this model. In [1,2] the dynamic case has been studied under the assumption of a uniform particle distribution. The effect of nonuniform particle concentration has been taken into account in [3], however only for the static case. The main objective of this work is to consider the influence of a nonuniform particle distribution on the stability of the magnetic fluid seal in the dynamic case.

Governing equations

The model consists of a system of partial differential equations, including the Maxwell' equations for the magnetic field strength, the Young-Laplace equation to describe the free surface, the Navier-Stokes-equation for velocity and pressure. An analytical solution for the magnetic field strength can be found due to the assumed hyperbolic shape of the polar head of concentrator. The three-dimensional Navier-Stokes-equation can be decoupled into a Laplace equation for the azimuthal velocity and a two-dimensional Navier-Stokes-equation for the secondary flow and pressure. The particle concentration is given by the convective-diffusion problem:

Find $C \in C^2(\Omega)$ such that:

$$-div\Big(\nabla C - (Pe\, v + \nabla(\ln\varphi))C\Big) = 0 \text{ in } \Omega,$$

$$\frac{\partial C}{\partial n} - C\frac{\partial}{\partial n}\ln\varphi = 0 \text{ on } \partial\Omega,$$

$$\frac{1}{|\Omega|}\int\limits_{\Omega} C\, dx = 1,$$

where v denotes the secondary flow and φ is a given function depending on the magnetic field strength.

Numerical solution of partial differential equations

The partial differential equations are discretized by finite elements of higher order. In particular,

- continuous, piecewise quadratic finite elements for the azimuthal velocity and for the particle concentration,
- continuous, piecewise quadratic finite elements enriched by cubic bubbles for the secondary flow,
- discontinuous, piecewise linear finite elements for the pressure.

The overall numerical algorithm consists of three sequential steps. The first step contains an iterations between Young-Laplace equation for the free surface shape and Laplace equation for the azimuthal velocity using known magnetic field strength. Then the calculations of the secondary flow with

known azimuthal velocity in fixed domain are coming. The last step containes computations of the particle concentration depending on the secondary flow.

It turns out that the problem for the particle diffusion is non-coercive which requires a nonstandard theory to guarantee existence, uniqueness and error estimates. It has been shown in [4] that this problem is well posed. Under certain regularity assumptions and for sufficiently small mesh sizes it was proved in [5] that the discrete problem has a unique solution, optimal error estimates in H^1 and L^2 were obtained.

Acknowledgments

The authors thank the German Research Foundation (DFG) for partially supporting this work by Graduate School 1554.

References

[1] V. Polevikov, L. Tobiska: Modeling of a Dynamic Magneto-Fluid Seal in the Presence of a Pressure Drop. Fluid Dynamics, Vol. 36, No. 6, 890-898 (2001).

[2] T. Mitkova, L. Tobiska: Numerical Simulation of the Flow in Magnetic Fluid Rotary Shaft Seals. Large-Scale Scientific Computing ed. by I. Lirkov, S. Margenov, J. Wasniewski, P. Yalamov, Lect. Note in Computer Science 2907, 396-403 (2004).

[3] V. Poleviov, L. Tobiska: Influence of diffusion of magnetic particles on stability of a static magnetic fluid seal under the action of external pressure drop. Commun Nonlinear Sci Numer Simulat 16, 4021-4027 (2011).

[4] Jérôme Droniu and Juan-Luis Vázquez: Noncoercive convection-diffusion elliptic problems with Neumann boundary conditions. Calculus of Variations 34:413-434 (2009).

[5] Susanne C. Brenner, L. Ridgway Scott: The Mathematical Theory of Finite Element Methods. Springer-Verlag, New York (2008).

Magnetic particles with shifted dipoles and magnetic rods: how the shape influences the microstructure.

M. Kilngkit[1], R. Weeber[1], E. Pyanzina[2], E. Krutikova, S. Kantorovich[1,2], C. Holm[1]

[1] *ICP, University of Stuttgart, Pfaffenwaldring 27, 70569, Stuttgart, Germany*
[2] *Ural Federal University, Lenin av. 51, 620083, Ekaterinburg, Russia*

Nowadays, when many of the magnetic fluid properties are well understood, various magnetic nanoparticles and colloids that deviate in one or another way from the spherical shape have been examined in recent years. Some examples are dumbbells, i.e. two overlapping spheres of opposite charges [1], magnetic core-shell particles [2], elongated ferroparticles [3], and colloidal particles with a magnetic cap [4]. In [5], we introduced and examined the ground states of a two-dimensional model system with magnetic particles, in which the dipole moment was shifted from the centre of the particle readially towards its surface. We call these particles sd-particles.

Sd-particles at Room Temperature.

We investigate here the magnetic and structural properties of sd-particles at room temperatures for various dipolar shifts. We reveal an unusual magnetization behaviour for high shift values. The combination of DFT and molecular dynamics simulations is employed to perform a cluster analysis. It turned out that to reproduce the experimental data from [4] for the ground states sd-particle model simplification is sufficient. However, in order to analyse tn detail the properties of capped colloids we calculeate the interaction potential for two magnetically caped colloids and compare it to the one of the two sd-particles.

Magnetic Rods.

The analysis of the interaction of two magnetic rods as a function of axes ratio is performed and preliminary results on the magnetization behaviour of the system of magnetic rods obtained theoretically and in molecular dynamic simulations are presented.

Conclusion

In this study we analyse the influence of the possible magnetic particles anisotropy on the macroproperties of the many-particle systems.

Acknowledgments

We are grateful for the financial support of MON s/c 02.740.11.0202, President RF Grant (MK-6415.2010.2) and Alexander von Humboldt foundation.

References

[1] G. Ganzenmueller and P.J. Camp. J. Chem. Phys., vol. 126 (2007), pp. 191104–191107.

[2] A.P. Philipse, M.P.B. van Bruggen and P. Pathmamanoharan. Langmuir, vol. 10 (1994), pp. 92–99.

[3] F. Vereda, J. Vicente and R. Hidalgo-Alvarez. Chem. Phys. Chem. , vol. 10 (2009), pp. 1165–1179.

[4] L.Baraban, D.Makarov, M.Albrecht, N.Rivier, P.Leiderer and A.Erbe. Phys. Rev. E, vol. 77 (2008), pp. 031407–031412.

[5] S. Kantorovich, R. Weeber, J. J. Cerda` and C. Holm. Soft Matter, DOI: 10.1039/c1sm05186e.

Experimental investigation on anisotropy of heat transport in magnetic fluids

M. Krichler, S. Odenbach

TU Dresden, Institute of Fluid Mechanics, Chair of Magnetofluiddynamics, 01062 Dresden, Germany

Introduction

Due to possible chain-like structure formation thermal conductivity k and thermal diffusivity a of some magnetic fluids are expected to depend on both, magnetic field direction and magnetic field strength [1]. Several experimental investigations are reported on this topic [2-4] but with a wide variety of results. In this work we present a different approach for the experimental setup of thermal conductivity measurements. Further on, we evaluate the results of measurements with several liquids to generate a heat transport model for magnetic fluids

Experimental setup

As far as published, for all former experiments the hot wire technique [5] was used. Thereby a thin wire is heated electrically and cooled by the surrounding liquid. Depending on temperature distribution thermal conductivity is determined. To study the thermal conductivity depending on strength and orientation of an external magnetic field, the field has to be aligned parallel and perpendicular to the heat flux. But there is no trivial possibility to align a magnetic field parallel to a radial heat flux.

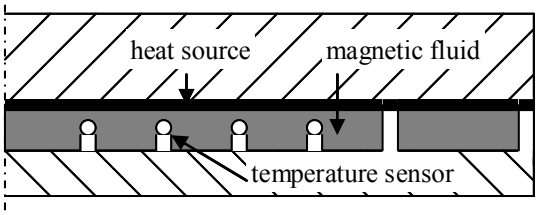

Figure 1: sketch with a cross-sectional view of the planar measurement device for thermal conductivity measurements.

Thus, this technique suffers from a lack of informative value to investigate the whole topic. Hence, we use a planar heat source for the measurement device (Fig. 1). This has the advantage that the magnetic field can be aligned in both directions to the heat flux, parallel and perpendicular. Furthermore, possible surface effects between the heat source or the temperature sensor and the liquid are reduced. In our setup thermal convection can be hindered by aligning the heat flux direction parallel to gravitation. With the aim of magnetic field homogenisation and segregation of potential thermal convection, due to thermal boundary effects, a permeable ring is included in the measurement device consisting of the sample liquid measured.

Results

First experimental results (Fig. 2) with ferrofluid TTR 630 confirm theory qualitatively [1].

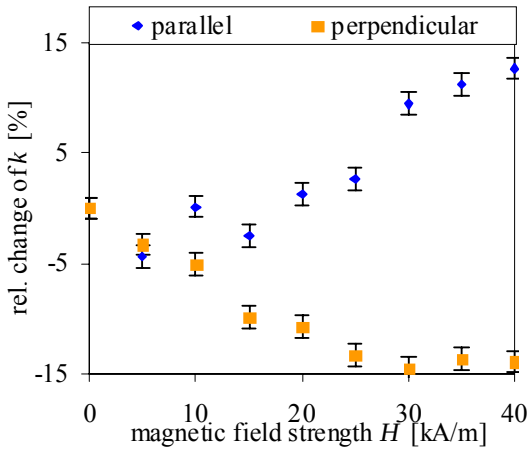

Figure 2: magnetic field depending change of thermal conductivity k of ferrofluid TTR 630

An increase of thermal conductivity is observed for parallel alignment of magnetic field and heat flux and a decrease for perpendicular alignment, vice versa. This experimental investigation is promising, since the measurement device allows a trustworthy interpretation of the obtained results.

Outlook

To investigate the heat transport mechanism in magnetic fluids in general measurements with further liquids which differ in particle size distribution and viscosity are carried out.

Acknowledgements

Financial support by *Deutsches Zentrum für Luft- und Raumfahrt* under grant number DLR 50 WM 0639 is gratefully acknowledged.

Special thanks are due to L. Vèkàs, Timişoara (Romania) for producing and providing the ferrofluid sample TTR 630.

References

[1] E. Blums, Journal of Magnetism and Magnetic Materials 252 (2002), 198

[2] Q. Li, Y. Xuan, J. Wang, Experimental Thermal & Fluid Sci. 30, 109 (2005)

[3] I. Djurek, A.Žnidaršič, A. Košak, D. Djurek, Croatica Chemica Acta 80, 3-4 (2007) 529

[4] J. Philip, P.D. Shima, B.Raj, Nanotechnology 19 (2008), 305706

[5] B.Ståhlhane, S. Pyk, Teknisk Tidskrift 61, 28 (1931) 389

Structure factors of polydisperse ferrofluids. Theory and simulations

E.Krutikova[1], S. Kantorovich[2], A.Ivanov[1]

[1] *Ural Federal University, Lenin av. 51, 620083, Ekaterinburg, Russia*
[2] *ICP, University of Stuttgart, Pfaffenwaldring 27, 70569, Stuttgart, Germany*

The ferrofluid properties are strongly dependent on its microstructure, which may be described by the pair correlation function, which means the probability density for the mutual position of two randomly chosen ferroparticles, the magnetic moments of which are averaged over all their orientations. The pair correlation function describes the interparticle correlations, which are responsible for the differences between the properties of a magnetic fluid and those of an ideal paramagnetic gas. Experimentally the structure properties of ferrofluids may be investigated with the small–angle neutron scattering technique [1]. Scattering measurements allows obtaining the so-called structure factor, which is actually the Fourier transform of the pair correlation function of the ferroparticle system. Thus, for correct processing of experimental data it is necessary to develop the theoretical model for the pair correlation function and structure factor. The ferroparticles of real magnetic fluids are distributed in sizes, so the particle polydispersity needs to be taken into account. In what follows, the virial thermodynamic perturbation method [2, 3] is used to calculate the pair correlation function of the magnetic fluid in the bidisperse approximation.

Thus, we have developed the theoretical model of polydisperse magnetic fluids within the bounds of bidisperse approximation. The comparison of the developed theoretical model with the results of molecular dynamics computer simulations showed good agreement.

Acknowledgments

This research was carried out under the financial support of the President of Russian Federation (Grants No. MK-2221.2011.2; MK-6415.2010.2) and the Ural Federal University (Grant No. 2.1.1/17). The research was also partly supported by the Ministry of Education and Science of Russian Federation; DAAD and Alexander von Humboldt foundation.

References

[1] D. Bica, L. Vekas, M.V. Avdeev, O. Marinica, V. Socoliuc, M. Balasoiu, and V.M. Garamus, Sterically stabilized water based magnetic fluids: Synthesis, structure and properties J. Magn. Magn. Mater. 311 (2007) 17-21.

[2] E.A. Elfimova, A.O. Ivanov, Pair correlations in magnetic nanodispersed fluids, J. Exp. Theor. Phys. 111 (2010) 146-156.

[3] J. Cerda, E. Elfimova, V. Ballenegger, E. Krutikova, A. Ivanov, C. Holm, Behavior of bulky ferrofluids in the diluted low coupling regime: theory and simulation, Phys. Rev. E 81 (2010) 011501-01-11.

In-situ study of iron oxide nanoparticle growth kinetics by means of magnetic particle spectroscopy

A. Lak, T. Wawrzik, H. Remmer, F. Ludwig, and M. Schilling

Institut für Elektrische Messtechnik und Grundlagen der Elektrotechnik, TU Braunschweig, Hans-Sommer-Str. 66, 38106 Braunschweig

1. Introduction

A deeper understanding of the magnetic particle growth kinetics in the nanometer regime is required for designing size controlled synthesis procedures. So far, research studies are primarily based on ex-situ monitoring of the particles growth reactions. These ex-situ studies are relied on taking aliquots from the reaction flask. For knowing the particle size distribution, a significant amount of the reaction mixture should be drawn for each aliquot. Undoubtedly, such excessive sampling not only disturbs and influences the growth kinetics, but also the aliquots in each step do not exactly represent the reaction state. Moreover, quantitative evaluation of a system over several hours growth reaction is a tedious process.
This report presents the real-time analyses of iron oxide nanoparticle formation and growth kinetics utilizing size dependent magnetic properties. Our own-built Magnetic Particle Spectrometer (MPS) setup [1] was combined with a room temperature iron oxide synthesis process and the particle's magnetic properties are extracted in-situ.

2. Particle synthesis procedure

In a typical synthesis procedure, potassium hydroxide solution (1 mol/L) was poured dropwise into a 200 mL iron (II) chloride (anhydrous, Aldrich) solution (0.1 mol/L) at room temperature till the pH value was adjusted to 7.9. Afterwards, the pH value was set to 7.5 by adding dropwise H_2O_2 solution (5.0 wt %). The final suspension was aged for 30 min in ambient atmosphere.

3. In-situ magnetic particle spectroscopy

In a typical in-situ measurement, the particle suspension is pumped continuously through the modified Magnetic Particle Spectrometer (MPS) setup in which the magnetization response of the particles to an applied sinusoidal excitation field of 9.96 kHz (field strength of 15 mT) is monitored. Subsequently, the particle's harmonic spectrum is obtained by Fourier transformation from the induced signal of the detection coil.
Furthermore, at each MPS measurement time, an aliquot was drawn from the particle synthesis suspension in order to be analyzed by fluxgate magnetorelaxometry.

4. Fluxgate magnetorelaxometry

Magnetorelaxometry (MRX) measurements were performed on a sample volume of 150 µL for a magnetizing field of 2 mT utilizing two fluxgate sensors in a differential configuration. Particle immobilization was conducted by freeze-drying the 150 µL suspension in mannite. In general, nanoparticle size distributions were obtained via the estimation of relaxation times. More details on the fluxgate MRX setup and the measurement analysis can be found in [2].

5. Results

A typical MPS spectrum of the reaction suspension aged for 4 min is shown in Fig. 1(a). The large number of odd harmonics indicates the formation of fairly big iron oxide nanoparticles. The temporal change of the spectral magnitude of the particles' odd harmonics is depicted in Fig. 1(b). The magnitude of the fundamental frequency of

the excitation signal remains constant during the whole recording period. As can be seen from Fig. 1(b) the spectral magnitude of higher harmonics rises steadily and hits maximum after 3-4 min growth. Based on the fact that an increase of harmonics spectral magnitude is correlated to a steeper M-H curve, it is proposed that the particle core sizes grow dramatically during the first minutes of aging. Afterwards, the higher harmonics spectral magnitude falls gradually over the reaction time whereas no significant change is observed in spectral magnitude of the third harmonic.

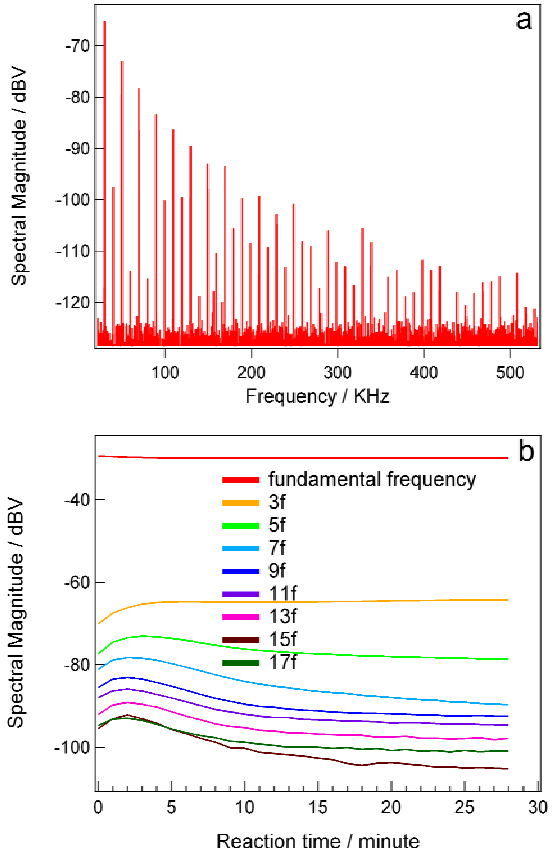

Figure 1: (a) Measured frequencies spectrum of iron oxide nanoparticle grown for four minutes (b) Temporal change of spectral magnitude of odd harmonics versus reaction time.

The Néel relaxation behavior of all taken aliquots was studied by performing MRX measurements. The information about core size and size distribution was extracted from the relaxation curves using the magnetic moment superposition model (MSM). The details about the model can be found in [3]. The obtained core size distribution parameters are shown in Fig. 2. As can be seen, the core size steeply rises during the first aging minute and then saturates at around 18 nm. The standard deviation drops from initially 0.3 to 0.15, and then it shows a slight increase with reaction time.
The constant spectral magnitude of the third harmonic after 4 min correlates with the unchanged core size. The slight increase of the standard deviation with reaction time may be responsible for the decay of the higher harmonic's spectral magnitude.

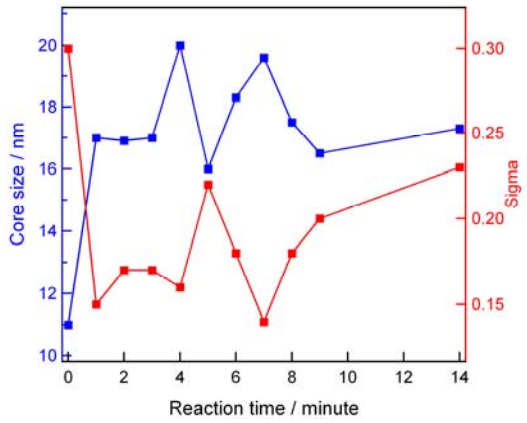

Figure 2: Core size distribution parameters of the sample aliquots obtained from MSM analyses.

6. Conclusion

It has been demonstrated that the modified MPS set up is an effective and reliable analysis method to trace iron oxide nanoparticle growth kinetics in-situ.

Acknowledgments

This work was financially supported by the DFG via SFB 578. Financial support by the International Graduate School of Metrology at Braunschweig (igsm) for PhD thesis (A.L.) is appreciated.

References

[1] T. Wawrzik et al., J. Appl. Phys (submitted).
[2] F. Ludwig et al., J. Magn. Magn. Mater. **321**, 1644 (2009).
[3] F. Ludwig et al., J. Appl. Phys. **101** 113909 (2007).

Patterns of thermomagnetic convection caused by short-wave modulation of the magnetic field

A. Lange and S. Odenbach

TU Dresden, Institute of Fluid Mechanics, Chair of Magnetofluiddynamics, 01062 Dresden, Germany

Introduction

Fluidic systems which are driven out of equilibrium by the temperature dependence of the density of the fluid belong to the set of classical pattern forming systems [1, 2]. By using a magnetic fluid (MF) as working substance new ways open up to generate patterns. The magnetization of the MF generates a magnetic force in interaction with an applied magnetic field which can also drive the system out of equilibrium. Thus, in a horizontal layer of MF subjected to a vertical gradient of temperature and a vertical magnetic field convection can be triggered in two different ways.
The study of thermomagnetic convection started with the consideration of static external magnetic fields [3–5]. Expanding the focus of interest, modulations of the magnetic field were first made with respect to time and lead to parametrically driven convection [6]. Alternatively, spatially modulated fields can be considered and are easy to to accomplish by placing sinus-like shaped iron bars in a constant magnetic field, see Fig. 1.

System

A laterally infinite horizontal layer of an incompressible layer of magnetic fluid of thickness d in the $x-y$ plane is bounded by two boundaries in the planes $z = \pm d/2$. The setup is heated from below with a temperature of T_b for the bottom boundary which results in a temperature difference of $\delta T = T_b - T_t$ with respect to the top boundary

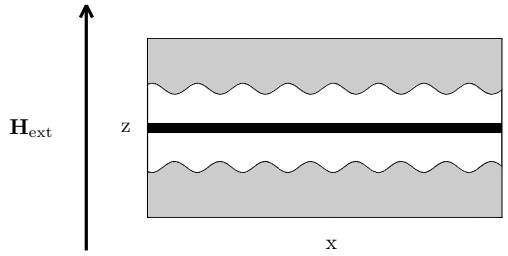

Figure 1: Symmetric arrangement of two sinus-like shaped iron bars (gray) beneath and above a centered layer of magnetic fluid (black) subjected to a vertical external magnetic field $\mathbf{H}_{\text{ext}}$. The white area indicates air.

with the temperature $T_t < T_b$. The layer is placed between two sinus-liked shaped iron bars and the entire system is subjected to a constant external magnetic field $\mathbf{H}_{\text{ext}} = (0, 0, H_{\text{ext}})$. Such a setup generates a nearly perfect vertical magnetic field which is modulated with the wavelength λ with respect to the horizontal coordinate x. The corresponding wave number k is given by $k = 2\pi/\lambda$.

Results

In the case of short-wave modulation, where $\bar{k} = kd \sim O(1)$ or larger holds, a pertubative ansatz as in [7] is not any longer possible to determine the base state for such a setup. Therefore a general ansatz has to be made which leads to a direct analytical solution of the problem. One known feature of the ansatz has to be that it recovers for vanishing modulation of the magnetic field the

quiescent base state with a linear temperature profile of the classical Rayleigh-Bénard setup. An ansatz fulfilling this constraint will be given as well as the general solution in its principle structure for the resulting set of differential equations.

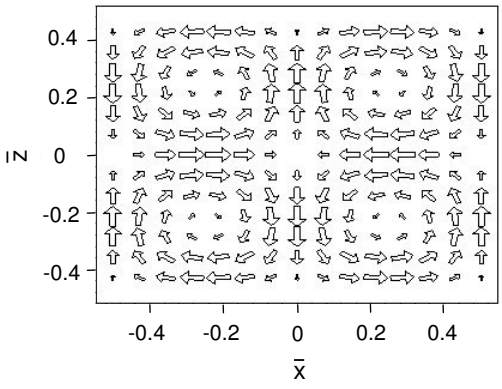

Figure 2: Plot of the flow field for a short-wave modulation with $\bar{k} = 2\pi$ and a scaled temperature difference of $\delta\bar{T} = 1$. Material parameters of APG 513A were used with $T_b = 30$ °C and $T_t = 20$ °C. The lengths are scaled with the thickness of the layer.

Figure 2 shows for $\bar{k} = 2\pi$ the characteristic feature of a double vortex structure which reflects the symmetrical modulations below and above the layer of fluid. The horizontal dimension of the convection roll is of the same size as its vertical, as one would expect from the basic convection pattern in the Rayleigh-Bénard system.
Thus the case of short-wave modulation emphasizes that the structure of the flow patterns follows directly the width of the modulation. If one applies a long-wave modulation, the pattern is stretched in x direction resulting in rather elongated rolls [7]. Contrary, for a short-wave modulation the pattern is given by more circular rolls. A detailed analysis of the calculated flow field is presented and compared to the features of the flow field for long-wave modulations. Furthermore, a suitable set of experimental parameters for an implementation of thermomagnetic convection caused by short-wave modulations is discussed.

References

[1] M. C. Cross and P. C. Hohenberg, Rev. Mod. Phys. **65**, 851 (1993)

[2] S. Chandrasekhar, *Hydrodynamics and hydrodynamic stability*, (1981)

[3] L. Schwab and U. Hildebrandt and K. Stierstadt, J. Magn. Magn. Mat. **39**, 113 (1983)

[4] L. Schwab and K. Stierstadt, J. Magn. Magn. Mat. **65**, 315 (1987)

[5] L. Schwab, J. Magn. Magn. Mat. **85**, 199 (1990)

[6] H. Engler and S. Odenbach, J. Phys.: Condens. Matter **20**, 204135 (2008)

[7] A. Lange and S. Odenbach, Phys. Rev. E **83**, 066305 (2011)

Shifting the Sol-Gel-Transition of a Hydroferrogel by Means of a Magnetic Field

P. Löwel[1], M. Krekhova[2], H. Schmalz[2], I. Rehberg[1], R. Richter[1]

[1]*Experimentalphysik V, Universität Bayreuth, 95440 Bayreuth, Germany*
[2]*Makromolekulare Chemie II, Universtität Bayreuth, 95440 Bayreuth, Germany*

Introduction

Smart chemically crosslinked gels with magnetic particles have been synthesized [1, 2], which can be controlled by external magnetic fields. In contrast to these permanent gels physical ferrogels are characterized by a reversible gelation, e. g. induced by pH or temperature changes. So far we have studied thermo-reversible organoferrogels [3] and hydroferrogels [4] using an ABA-type triblock copolymer as gelator. For the case of hydroferrogels we use a Pluronic^{TM} P123 gelator in combination with water-based ferrofluids. The latter gels are "inverse-gels", i. e. liquid at low temperatures, whereas gelation occurs at elevated temperatures. For details of the rheological behaviour and the phase diagram reconstructed therefrom see Ref. [4]. In the following we investigate for the first time the influence of the magnetic field on the temperature induced sol-gel-transition for a gel with 35 wt % gelator, which is based on a magnetic liquid with 5 wt % cobalt ferrite.

Rheology

A rotational rheometer (MCR301, Anton Paar) with the commercial magnetorheological device (MRD 170/1T) and a coaxial parallel plate system with a diameter of 20 mm (PP 20/MR) was used. The gap between the bottom and top plate was selected to be 1 mm. In all cases the applied magnetic induction was measured by means of a Hall-probe positioned 1 mm underneath the filled gap. Prior to filling the ferrogel was cooled in ice water and then transferred to the gap by means of a syringe. Before starting with the measurement the sample was presheared. Then the storage- (G′) and loss modulus (G″) were investigated via the oscillatory mode. These quantities were investigated by increasing the temperature by 0.3 °C every three minutes.

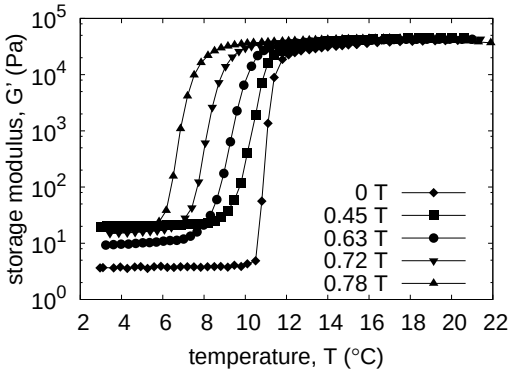

Figure 1: Storage modulus versus temperature for different values of the applied magnetic induction.

Results

We have measured the storage and loss modulus versus the temperature for nine values of the magnetic induction. Figure 1 shows five exemplary curves for the storage modulus. For zero magnetic induction one observes a steep increase of G′ over four decades at around 11 °C (see filled rhomboids). Increasing the magnetic induction this transition is shifted

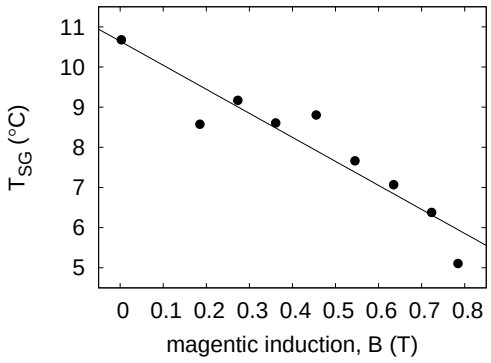

Figure 2: Sol-gel-transition temperature T_{SG} versus applied magnetic induction. For convenience we display a fit by $T_{\mathrm{SG}}(B) = a \cdot B + T_0$, with $a = (-5.98 \pm 0.83)\,\frac{\mathrm{K}}{\mathrm{T}}$, $T_0 = (10.64 \pm 0.42)\,^{\circ}\mathrm{C}$.

to lower temperatures. For the maximal applied induction of 0.78 T the transition takes place at 5 °C (see filled triangles). For a quantitative estimate of the transition point T_{SG} we resort to a phenomenological description of $G'(T)$. We fitted the measured data by means of the logistic curve [5] which is charaterises self limiting growth processes. The point of inflexion of the logistic function serves as an estimate for T_{SG}. In Figure 2 we plot T_{SG} versus the applied magnetic induction. Within the resolution of the measurement we observe a linear decay of T_{SG} by $6\ \mathrm{K} \cdot \mathrm{T}^{-1}$.

It is well known that the cobalt ferrite particles form chains in an external magnetic field [6, 7]. By inspecting G′ in the sol regime we conclude that a magnetorheological explanation is not sufficient to explain the shift of the transition. A possible explanation might be that the particle chains serve as seeds for the gelation process. Alternatively the chains might bridge gaps between neighbouring gel clusters and in this way facilitate the gelation process.

Acknowledgments

The authors thank H. R. Brand for friutful discussions. Financial support by the German Research Foundation (DFG) via the corporate research center FOR 608 is gratefully acknowledged.

References

[1] M. Zrinyi, Trends in polymer science (Regular ed.) **5**, 280 (1997).

[2] M. Zrinyi, Colloid. Polym. Sci. **278**, 98 (2000).

[3] G. Lattermann and M. Krekhova, Macromol. Rapid. Commun. **27**, 1373 (2006), see *ibid.* 1968 for the *erratum.*

[4] M. Krekhova, T. Lang, R. Richter, and H. Schmalz, Langmuir **26**, 19181 (2010).

[5] D'Arcy Wentworth Thompson, *On Growth and Form* (Cambridge University Press, Cambridge U. K., 1942).

[6] S. Odenbach, *Magnetoviscous Effects in Ferrofluids* (Springer, Berlin, Heidelberg, New York, 2002).

[7] P. Ilg and S. Odenbach, in *Colloidal Magnetic Fluids: Basics, Development and Applications of Ferrofluids*, edited by S. Odenbach (Springer, Berlin, Heidelberg, New York, 2009), Vol. 763, Chap. 4, pp. 238–301.

Magnetic nanoparticles functionalized with Mitoxantron in cell culture – a Real-time cell analysis (RTCA)

S. Lyer*, S. Dürr*, J. Mann, R. Tietze, E. Schreiber, C. Alexiou

*The authors contributed equally to the work.

Department of Oto-Rhino-Laryngology, Head and Neck Surgery, Section for Experimental Oncology and Nanomedicine (SEON), Else Kröner-Fresenius-Stiftung-Professorship, University Medical Center Erlangen, Germany

Introduction:

Magnetic Drug Targeting (MDT) is a new and innovative approach in cancer treatment. To avoid the adverse effects of chemotherapy, the therapeutic agent is linked to superparamagnetic nanoparticles, which are injected into a tumor supporting artery and focused by an external magnetic field to the tumor region, to have a maximum local impact. Analysis of nanoparticles and the chemotherapeutic substance (e. g. Mitoxantrone) in human cancer cell culture (e. g. MCF-7) is necessary to gain respective informations for *in vivo* applications.

Methods:

The effect of pure Mitoxantrone (MTO) and MTO bound to nanoparticles was tested on human cancer cell lines using Real-Time Cell Analysis (RTCA) and LDH-Assay. RTCA is performed by impedance-measuring. The impedance is expressed in the Cell Index (CI), which is a parameter for cell viability.

Results:

RTCA showed that MTO bound to functionalized nanoparticles was more toxic than the drug alone. The CI is clearly faster decreased by adding the chemotherapeutics bound to functionalized nanoparticles than adding the pure drug. However, in first experiments the particles themselves showed no toxicity in therapeutically relevant concentrations. These results could be confirmed by LDH-Assay.

Conclusion:

The toxic effect of chemotherapeutic agents (e. g. Mitoxantrone) on human cancer cell lines (e. g. MCF-7) can be enhanced, if these drugs are bound to magnetic nanoparticles. These preliminary data show a dependency of these different application modes by RTCA. The results are a first step for a better understanding of the effectiveness of MDT as a new and innovative cancer treatment.

Acknowledgements:

DFG (PAK 151), Else Kröner-Fresenius-Stiftung, Bad Homburg v.d.H.

How fast can a magnetic snake swim on the water?

F. J. Maier[1], I. Rehberg[1], R. Richter[1]

[1] *Experimentalphysik V, Universität Bayreuth, 95440 Bayreuth, Germany*

Introduction

Objects floating on the interface between a liquid and a gas, like bubbles on your cup of hot chocolate, tend to self-assemble due to capillary interaction [1]. For floating magnetic microparticles one can additionally impose a repulsive dipole-dipole interaction by means of a magnetic field oriented normally to the surface. This may result in a hexagonal lattice of particles. Even more complex patterns are formed under influence of an alternating magnetic field. Supported by capillary surface waves the magnetic microparticles self-assemble into patterns, which might resemble snakes [2]. Large-scale vortex flows propel asymmetric snakes to move around erratically [3]. Symmetric snakes can be transformed to asymmetric ones, by attaching a floating objects to one side of the snake [3]. In our study we present measurements of the swimming velocity of magnetic snakes attached to a floating disc.

Experimental setup

Spherical nickel particles of ≈ 90 μm diameter are dispersed on the surface of deionized water. They float due to surface tension. For the experiments a circular glass dish of 70 mm diameter and 11.5 mm depth is used. We fill the vessel with deionized water to a level of 8 mm, which yields a concave meniscus at the container edge. The dish is placed in the midplane of a Helmholtz pair of coils, connected to a power supply, as sketched in Fig. 1. We generate a sinusoidal modulated field with a driving frequency f between 50 and 150 Hz, and an amplitude ΔB of up to 14 mT. In the experimental area the field is homogeneous with 97 % accuracy. The structures are observed from above by a charge-coupled-device video camera (Lumenera) which is connected to a computer. For illumination we utilize an electroluminescent film mounted below the transparent vessel. For details of the setup see Ref. [4].

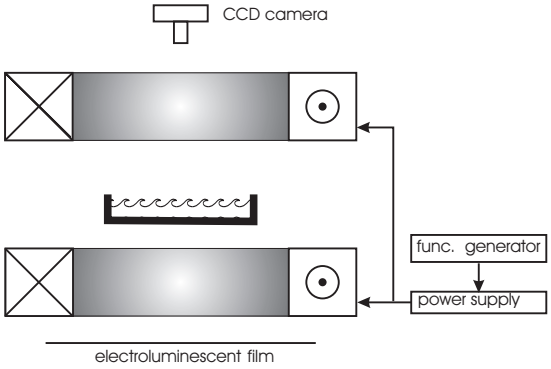

Figure 1: Sketch of the setup.

After distributing micro particles on the liquid surface, the driving amplitude ΔB is carefully increased, until a magnetic snake evolves. Then a plastic disc is positioned on the liquid surface next to the snake by means of a pair of tweezers. The disc is floating due to surface tension and therefore self-attaches to one end of the snake because of capillary interaction [1], creating a snake-disc hybrid. The utilized discs are washers having an outer diameter of 5.5 mm, an inner bore of 2.4 mm, and a height of 0.5 mm.

Results

The snake-disc hybrids are swimming in the direction of the disc-head, with the

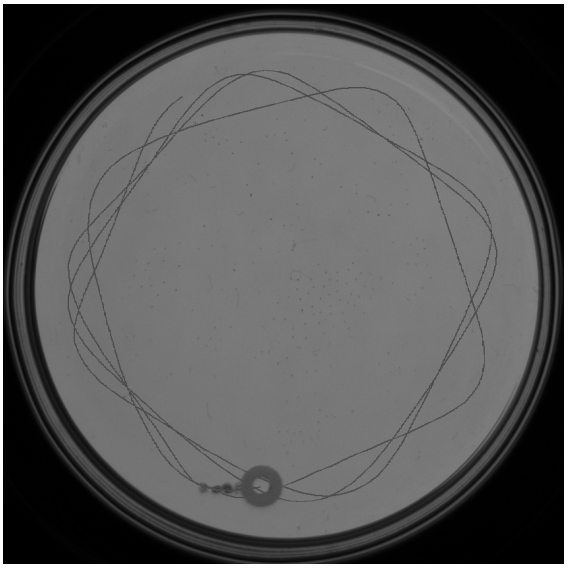

Figure 2: Trace of a snake-disc hybrid, recorded for 30 s, at a driving amplitude (RMS) of $\Delta B = 12$ mT, and a driving frequency of $f = 80$ Hz. Exposure time is 15 ms.

snake as a tail. Figure 2 displays a hybrid in the dish, together with its trace, recorded via object tracking. The trace consists of straight parts, which are connected by curves. In the curves the snake-disc hybrid is deflected from its intrinsic course by the meniscus next to the container edge. We observe quasiperiodic curves, like in Fig. 2, as well as simple circular traces (not shown here). The latter occur, when the hybrid swims alongside the edge of the dish. The diameter of such a circular trace increases with the driving amplitude, reminiscent of the diameter of a bicycle course in a velodrome.
We have measured the swimming velocity of the snake-disc hybrids for different values of the driving amplitude and frequency. Figure 3 presents the results for varying driving amplitude and a constant driving frequency. The solid line stems from a fit by the model put forward in Ref. [3]

$$v = \text{const} \cdot \frac{f \cdot \Delta B^2}{a_0}. \qquad (1)$$

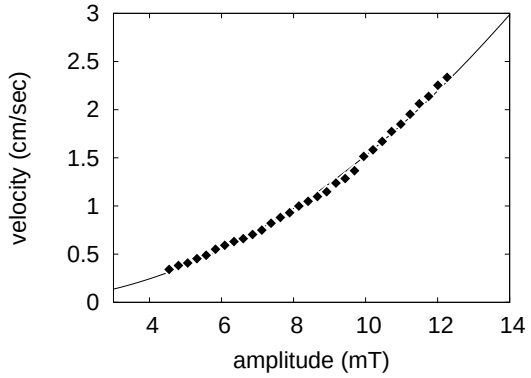

Figure 3: Swimming velocity versus amplitude of the driving magnetic induction and a driving frequency of $f = 80$ Hz.

Here a_0 denotes the characteristic length of a snake segment. The experimental data are well described by the quadratic Eq. (1).
Moreover we investigate in our contribution $v(\Delta B)$ for different snake-disc hybrids. Eventually we study the frequency dependence of the swimming velocity.

Acknowledgments

The authors thank A. Snezhko for fruitful discussions.

References

[1] D. Vella and L. Mahadevan, Am. J. Phys. **73**, 817 (2005).

[2] A. Snezhko, I. S. Aranson, and W.-K. Kwok, Phys. Rev. Lett. **96**, 078701 (2006).

[3] A. Snezhko, M. Belkin, I. S. Aranson, and W.-K. Kwok, Phys. Rev. Lett. **102**, 118103 (2009).

[4] A. Baumgärtner, Diplomarbeit, Experimentalphysik V, Universität Bayreuth, 2011.

Hybrid Polymeric Nanostructures for Biomedical Applications

G. U. Marten[1], T. Gelbrich[2], H. Ritter[3], A. M. Schmidt[1]*

[1] *Department Chemie, Universität zu Köln, Luxemburger Str. 116, D-50939 Köln,* [2] *present address: Qiagen GmbH, Hilden,* [3]*Heinrich-Heine-Universität Düsseldorf, *E-Mail: annette.schmidt@uni-koeln.de*

Defined hybrid nanomaterials that are available by the combination of inorganic and organic nanoscopic building blocks typically show a combination of the properties of the single compounds, or even fully new functions. Especially in the biomedical field, they provide new opportunities for special applications, like drug delivery, bioseparation and biocatalysis. In our work we present hybrid core-shell nanostructures with a customized properties profile, consisting of magnetic cores, decorated with a biocompatible polymer brush shell that can be used for different biomedical applications. By implementing magnetic cores, a remotely controlled stimuli responsive system can be obtained with the potential of external manipulation, e.g. for separation purposes, and local heating by HF irradiation.

The main component of the polymer shell is based on oligo(ethylene glycol) methylether methacrylate (OEGMA) monomers exhibiting ethylene glycol side chains of varying length,[1] combined with functional comonomers for biofunctionalization. The grafted polymer arms are formed by surface-initiated atom transfer radical polymerization (SI-ATRP) and prevent agglomeration by steric stabilization with great dilution stability.[2] Due to the lower critical solution temperature (LCST) of POEGMA in water, that can be tailored by the polymer composition, the core-shell nanoparticles show a thermoresponsive dispersion behavior.

Additional functional groups like active esters (*N*-hydroxysuccinimide, SI) and nanocontainers (β-cyclodextrin, CD) can be covalently introduced into the particle shell by copolymerization with functional methacrylates, thus providing a highly modular system.

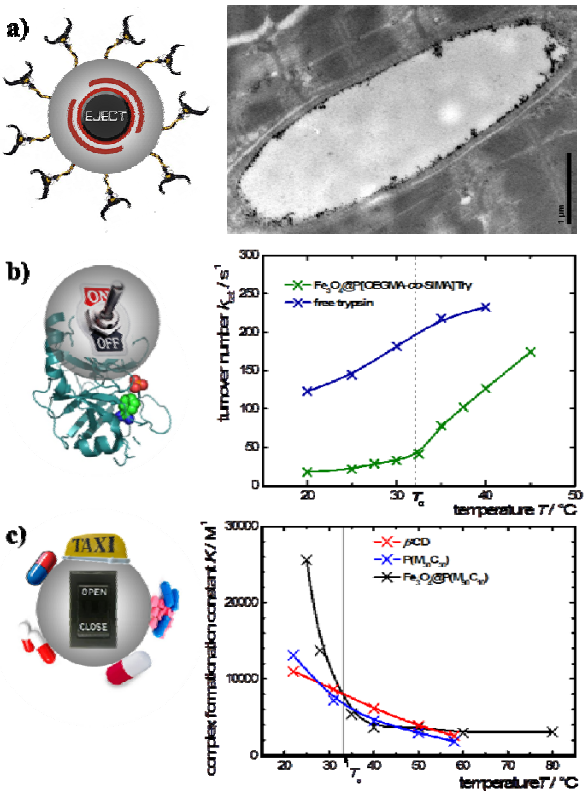

Fig. 1: Functional hybrid particles for: a) labeling of membrane proteins and cells, b) active biocatalysis with immobilized enzymes, c) drug delivery on demand

Accordingly, the hybrid nanoparticles can be tailor-made for several applications in biomedicine, e. g. bioseparation,[3] biocatalysis[3,4] and drug delivery.

Selective and controlled separation of specific substances is a common task in the biomedical field. For this purpose magnetic beads with various functionalities are commercially available however, they are mostly multi-core microspheres, consisting of magnetic nanoparticles in a functional

polymer shell. These microspheres possess a high susceptibility, providing a fast separation in low magnetic field gradients. In contrast, single cored nanoparticles imply a high surface to volume ratio, leading to a high specific functionalization density. On the other hand, they are difficult to separate due to low susceptibility, and Brownian motion. To achieve a combination of both advantages, we exploit the thermoresponsive effect of active ester-functional P(OEGMA-*co*-SIMA) shells. SI-functional nanohybrids are shown to effectively label membrane proteins (s. Fig. 1a) in order to isolate and characterize them via protein analysis.

Enzyme catalyzed reactions are often used in organic and biological syntheses. The enzymes are often costly, and so catalyst recovery is an interesting option. By immobilizing enzymes within the polymer brush shell of P(OEGMA-*co*-SIMA)-coated magnetic nanohybrids, they become magnetically separable and furthermore it is shown that the enzyme activity of this quasi-homogeneous magnetic biocatalytic system can be reversibly controlled by heating with HF irradiation (s. Fig. 1b).

Drug delivery is a highly discussed field of research in biomedicine. By restricting drug exposure only to the diseased part of the body, side effects can be minimized. Currently there are diverse approaches for this problem; one of them is guiding magnetic carriers to the diseased region by field gradients (magnetic drug targeting). For active drug delivery purposes, core-shell nanoparticles functionalized with cyclodextrin units can be used to reversibly bind and release small molecule drugs. In certain cases, the complex formation can be highly temperature sensitive due to entropic effects leading to release burst upon heating.

The magnetic cores can be manipulated by a magnet for drug targeting. The opportunity of magnetic heating in an HF-field permits the remote controlled release of the drug on demand (s. Fig. 1c).

Acknowledgments

We thank Prof. J. Schrader, Universitätsklinikum Düsseldorf and Dr. M. Reinartz for cell membrane labeling tests. For financial support, we acknowledge the DFG (Emmy-Noether-Programm) and the FCI (A. M. Schmidt, G. U. Marten)

References

[1] T. Gelbrich, G. U. Marten, A. M. Schmidt, *Polymer* (51), 2818-2824, **2010**.

[2] T. Gelbrich, M. Feyen, A. M. Schmidt, *Macromolecules* 39, 3469-3472, **2006**.

[3] T. Gelbrich, M. Reinartz, A. M. Schmidt, *Biomacromolecules* 11(3), 635-642, **2010**.

[4] G. U. Marten, T.Gelbrich, A. M. Schmidt, *Beilstein Journal of Organic Chemistry* 6, 922-931, **2010**.

Field dependent Measurements of the Specific Absorption Rate

R. Müller[1], S. Dutz[1], A. Neeb[2], M. Zeisberger[3]

[1] *Department of Nano Biophotonics, Institute of Photonic Technology, Jena, Germany*
[2] *Karlsruhe Institute of Technology, Karlsruhe, Germany*
[3] *Department of Spectroscopy and Imaging, Institute of Photonic Technology, Jena, Germany*

Magnetic iron oxide nanoparticles (MNP) are promising tools for medical applications like hyperthermia. The relevant property (specific absorption rate or heating power SHP) depends not only on particle size, size distribution and microstructure but as well on AC magnetic field conditions.
There are several mechanisms to reverse the direction of magnetization of a MNP in an AC field: Brown relaxation, Néel relaxation and ferromagnetic hysteresis. During a SHP measurement their superposition leads to a temperature increase in the particles. The influence of the mean particle size on hysteresis losses and switching behaviour could be already shown in [1, 2]. In these cases SHP-measurements were only carried out at one certain field amplitude. Field dependent SHP measurements couldn't be found in literature. The most investigations cover field amplitudes what are not sufficient for hysteretic MNP.

Small single domain particles were prepared by a precipitation of NPs from iron chloride solution by means of KOH. The samples SD1 and SD2 differ in the addition rate of the KOH-solution. Multi core NP (MCNP) were prepared by a slow precipitation with $NaHCO_3$ [3]. They have a raspberry-like structure. Large single domain particles LSDP were prepared similar to [4]: Into a NaOH solution NaNO3 as an oxidant was added. $FeCl_2$ solution was added and the mixture was kept at 25°C for 24 h. Coating experiments were carried out with carboxymethyldextran [3]. The suspensions of MCNP and LSDP sedimentate within some hours (LSDP) and several days (MCNP), respectively. LSDP show a XRD-pattern close to that of Fe_3O_4 whereas MCNP, SD1 and SD2 are more or less maghemite. From the XRD pattern (Fig.1) a mean crystallite size was estimated using the Scherrer formula.

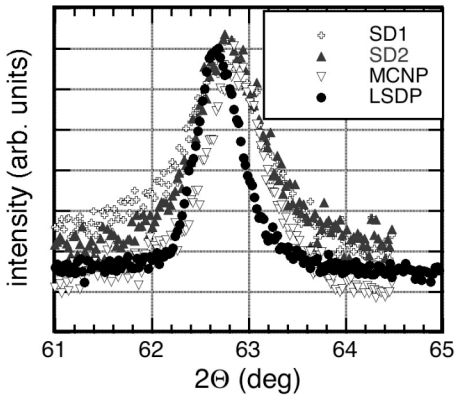

Figure 1: XRD pattern (440 peak)

Our samples consist of a certain fraction of superparamagnetic particles which is indicated by a reduced remanence and of hysteretic particles what are characterized by the switching field distribution *S(H)* (amount of particles which switch their magnetization irreversibly at the field *H*). *S(H)* was calculated from initial remanence curves and fitted by a log-normal distribution [5].
Specific hysteresis losses (SHL) at different maximum field strengths were calculated from minor loops. All magnetic measurements were carried out by a vibrating sample magnetometer MicroMag™ 3900 (Princeton Measurements Corp., USA).
For the calorimetric determination of SHP the suspensions were thermally isolated and placed into a coil what provides the magnetic field (f = 210 kHz, *H* up to 30 kA/m). Heating curves were measured with a fibreoptical sensor. The field generator is based on a HTG-10000 device by Linn

HighTherm, Germany. SHP was calculated by multiplying the specific heat capacity of the sample, 1/mass concentration (from M_S-values) and the heating rate determined after switching on the field.

Tab. 1 shows the development of hysteresis properties with XRD crystallite size. MCNP consist of subgrains with the given size. Investigations of single crystalline particles [1] have shown that MCNP reveal a smaller hysteresis (H_C) than single crystalline NP with comparable crystallite size. M_S of SD1 and SD2 is typically for γ-Fe_2O_3-NPs. The lower value of MCNP might result from a small fraction of non-magnetic iron oxide. The high value of LSDP indicates that the sample consists of a mixture of γ-Fe_2O_3 and Fe_3O_4 what corresponds with a XRD peak shift.

Tab. 1. Magnetic parameters of dried powders (H_C: coercivity [kA/m], m_{rs}: M_{rs}/M_s, M_s: spec. magnetization [Am^2/kg], H_m: mean value of S(H) [kA/m], σ: width of *S(H)*), d_{XRD} [nm]

sample	H_c	m_{rs}	Ms	H_m	σ	d_{XRD}
SD1	0.83	0.018	64.9	11.4	0.820	10.9
SD2	1.2	0.033	66.8	9.8	0.836	12.6
MCNP	4.0	0.084	59.5	14.1	0.609	15.2
LSDP	11.2	0.122	79.9	26.2	0.611	20.5

SHL were investigated because they are the dominant mechanism in bigger particles. Comparing SHL per magnetization cycle multiplied by frequency used for the calorimetrically measured SHP-values the contribution of SHL on the SHP can be estimated for investigated field amplitudes. The field strength at which saturation behaviour starts corresponds roughly with H_m of *S(H)*. There is only a weak influence of H_C on SHL at low fields (H_{max}<5 kA/m). As well the small mean crystallite size, the low m_{rs} < 0.5 even for LSDP as the analysis of *S(H)* suggest the influence of a fraction of small particles what corresponds with the fact that "Stoner-Wohlfarth like" particles show negligible hysteresis losses at low field amplitudes $H<H_c$ [2].
SD1 and SD2 reveal SHL in the order of only < 10% and < 25%, respectively, of the measured SHP. The MCNPs possess SHL of about 50 – 60% of the total losses whereas in LSDP hysteresis losses are clearly dominant. The slope of SHP as well as hysteresis losses with increasing field amplitude of SD1 is close to a H^2-dependence what is an indication for Neel relaxation.
LSDP behave closer to blocked single domain (Stoner-Wohlfarth) particles what show a theoretical limit of losses per cycle of 7 J/kg (≈1400 W/g @210kHz) [2].
It is noticeably that the hysteresis losses of all samples reveal their saturation already at lower field amplitudes than the SHP. In case of MCNP and in particular LSDP no indication of any saturation behaviour can be seen at 30 kA/m. The SHP of MCNP is about 600 W/g at 30 kA/m.

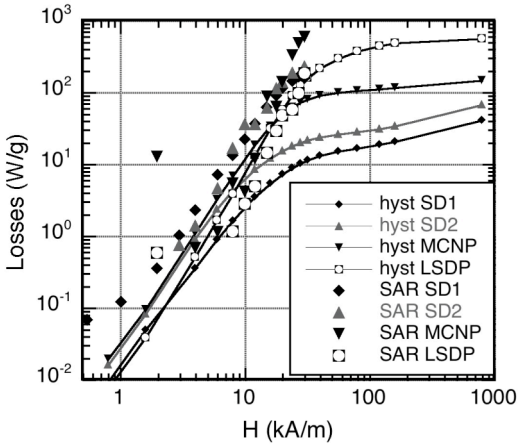

Figure 2: Comparison of hysteresis losses and SLP of different types of particles

Acknowledgments

The authors gratefully acknowledge financial support by the EU and DFG (Project 214137 NANO3T and ZE825/1-1).

References

[1] R. Müller et al., J.Magn.Magn.Mater. 323 (2011) 1223-1227

[2] R. Hergt et al., J. Phys.: Cond. Matter 18, 2919-34 (2006).

[3] S. Dutz et al., J. Magn. Magn. Mater. 321/10: 1501-1504 (2009).

[4] K. Nishio et al., Magn. Magn. Mater. 310 (2007) 2408–2410

[5] M. Zeisberger et al., J. Phys.: Conf. Series **149** (2009) 012115

Semi-quantitative XμCT analysis of nanoparticle content in biological tissue samples after magnetic drug targeting.

H. Rahn[1], S. Lyer[2], D. Eberbeck[3], F. Wiekhorst[3] L. Trahms[3], Ch. Alexiou[2] and S. Odenbach[1]

[1] *Chair of Magnetofluiddynamics, Technische Universität Dresden, Dresden 01062, Germany*
[2] *ENT-Department of the University Erlangen-Nürnberg, Section for Experimental Oncology and Nanomedicine (Else Kröner-Fresenius-Foundation-Professorship), Waldstr. 1, 91054 Erlangen, Germany*
[3] *Physikalisch-Technische Bundesanstalt, Berlin, Germany"*

Magnetic nanoparticles are used as drug carriers for the minimal invasive cancer treatment magnetic drug targeting (MDT) [1, 2]. This minimal invasive treatment has been studied on animal models, such as tumour bearing rabbits and an ex-vivo artery model [3].

For the success of MDT the magnetic nanoparticles carrying drugs should be distributed in the tumour with a well defined homogeneous concentration.

X-ray microcomputed tomography (XμCT) has been introduced as a capable method to study the nanoparticle distribution in biological tissue samples. The results are 3-dimensional representations of the nanoparticle accumulation with a spatial resolution of few micrometers. [3, 4]. But the polychromatic nature of the X-ray beam complicates a quantitative examination of the tomographic data. Thus, the tomogramms of complex multi-phase soft tissue samples can be evaluated in a qualitative way only.

Magnetorelaxometry (MRX) is a very sensitive method for magnetic nanoparticle detection with a mass resolution of several nanograms but providing only a poor spatial resolution [5].

To achieve a semi-quantitative evaluation of tomographic data sets few methods can be used. These are for example calibration, dual-energy tomography and phase contrast tomography.

In case of the laboratory XμCT apparatus LeTo the calibration has been chosen. Therefore a phantom system has been developed as there were no adequate phantoms available. Following requirements for the new phantom has to fulfill:

- the body material has to be an acceptable substitute for biological tissue
- two component system
- the nanoparticle concentration is the only variable
- long-term stable

An elastomere polyurethan (PUR) gel has been chosen as body material as it is an accepted substitute for body tissue in radiologic imaging [6]. Magnetic nanoparticles are suspendable in the elastomere. It can be casted to any shape and after curing it is long-term stable. For the calibration six phantoms with different nanoparticle concentration from 0 mg/ml to 35 mg/ml have been prepared. Figure 1 shows an example of a PUR-ferrofluid gel.

Figure 1: Two rectangular PUR-ferrofluid-gels

The phantoms have been measured by means of XμCT and reconstructed under the same boundary conditions. The analysis of the tomographic data sets yields a mean grey value for each nanoparticle concentration. Further on, the phantoms have been analysed magnetically using a vibrating sample magnetometer. Here, the nanoparticle concentrations have been detected experimentally. The mean grey values as well as the nanoparticle concentrations have been combined to a calibration curve shown in Figure 2.

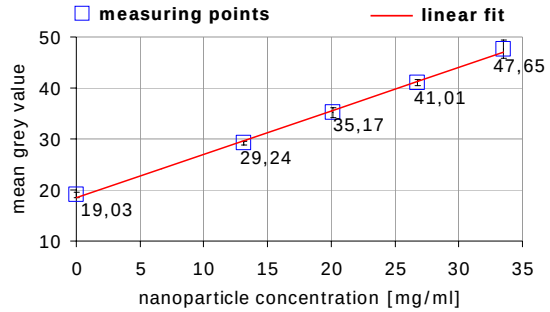

Figure 2: Calibration curve for the polychromatic tomography equipment LeTo for particular boundary conditions.

For the semi-quantitative analysis a special software has been created. This software connects the grey values available in the tomogram to nanoparticle concentrations. The results are on the one hand an image stack where the nanoparticle concentrations are connected to assigned colours and on the other hand a table with nanoparticle concentrations.

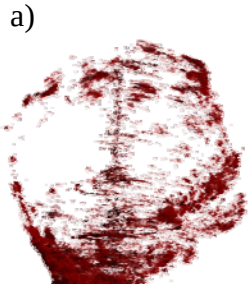

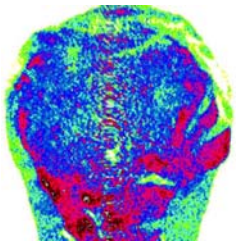

c)

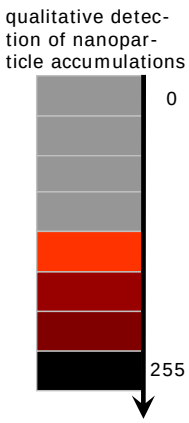

d)

concentration [mg/ml]

von	bis	von	bis
0.0	1,0	14,0	15,5
1,0	2,0	15,5	17,0
2,0	4,0	17,0	18,5
4,0	6,0	18,5	20,0
6,0	8,0	20,0	22,5
8,0	9,5	22,5	25,0
9,5	11,0	25,0	27,5
11,0	12,5	27,5	30,0
12,5	14,0	30,0	32,5
14,0	15,5	32,5	35,5

Figure 3a) and c): qualitatively examined tumour after MDT and corresponding colours representing the nanoparticle amount b) and c): the same tumour but evaluated in a semi-quantitative way, thereby the different colours correspond to nanoparticle concentrations.

Both evaluation ways show a preferential accumulation of magnetic nanoparticles in the border regions of the tumour. Additionally, the semi-quantitative analysis reveals that the nanoparticle content of this tumour amounts to 24.41 mg.
Magnetorelaxometry results have been used as a reference. Here the detected nanoparticle content is 25 mg. The calculated deviation between the semi-quantitative tomographic results and quantitative MRX-results amounts to 2.36 %.
In the future several conditions for the tomographic imaging will be tested. This enables a semi-quantitative evaluation of already measured objects.

Acknowledgments

These studies are supported by the Deutsche Forschungsgemeinschaft (DFG-OD 18/16-1 and TR 408/5-1).

References

[1] C Alexiou, W Arnold, RJ Klein, FG Parak, P Hulin, C Bergeman, W Erhardt, S Wagenpfeil; (2000) Locoregional cancer treatment with magnetic drug targeting. Cancer Research 60:6641-6648

[2] R Jurgons, C Seliger, A Hilpert, L Trahms, S Odenbach and Ch Alexiou; J. Phys.: Condens. Matter 18 (2006) S2893–S2902

[3] R Tietze, H Rahn, S Lyer, E Schreiber, S Odenbach, C Alexiou; Journal: Histochemistry and Cell Biology, 135, 2 (2011)153-158

[4] H Rahn, I Gomez-Morilla, R Jurgons, Ch Alexiou, D Eberbeck, S Odenbach; Journal of Magnetism and Magnetic Materials 321 (2009) 1517–152

[5] H Richter, F Wiekhorst, K Schwarz, S Lyer, R Tietze, Ch Alexiou and L Trahms; Phys. Med. Biol. 54 (2009) N417–N424

[6] C B Chiarot, J H Siewerdsen, T Haycocks, D J Moseley and D A Jaffray, Physics in Medicine & Biololgy 50 (2005) N287 - N297

Nanorheological approach using magnetically blocked $CoFe_2O_4$ nanoparticles in polymer solutions

E. Roeben[1], R. Messing[1], A. M. Schmidt[1,*]

[1] *Institut für Physikalische Chemie, Universität zu Köln, Luxemburger Straße 116, D-50939 Köln*

Microrheology, thus techniques to investigate the rheological properties of soft matter by means of colloidal tracer probes, is achieving recent advancement. One can distinguish between passive and active microrheological methods. In passive microrheology, the inherent thermal energy is used to move the tracers.[1,2] In active microrheology the embedded probe is actively driven within the material, either in oscillatory or steady motion. Possible driving forces are gravity, laser tweezers or magnetic fields. The use of magnetic gradients to move magnetic particles has attracted considerable interest in this context. Recently is has been shown that particle rotation in static or oscillatory fields can be used to get information about particle-matrix-interaction.[3]

The goal in the presented work is to investigate rheological properties of complex fluids like polymeric matrices by analyzing the magnetic behavior of embedded magnetic particles in static and dynamic magnetic fields. Our model systems for this purpose are aqueous polyacrylamide (PAAm) solutions containing magnetically blocked $CoFe_2O_4$ nanoparticles (Fig. 1) as tracing particles.

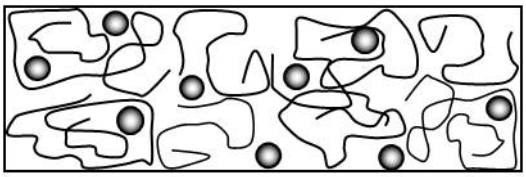

Figure 1: $CoFe_2O_4$ nanoparticles embedded in PAAm-solution.

The different concentrated samples are analyzed using Vibrating Sample Magnetometry (VSM) and AC susceptometry (Fig. 2). The local viscosity η experienced by the magnetic particles is obtained from AC susceptometry experiments and is compared to macroscopic related results received in static and dynamic rheological measurements using conventional rheological methods. By comparing the results of the different methods we get information about the correlation between the local viscosity around the particles and the macroscopic viscosity.

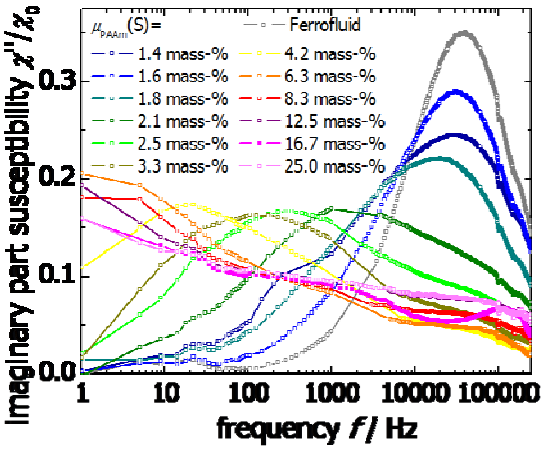

Figure 2: AC-susceptometry for different concentrated samples of PAAm.

Acknowledgments

We acknowledge the Deutsche Forschungsgesellschaft (DFG) for financial support within in the framework of SPP 1259 “Intelligent Hydogels”.

References

[1] T. M. Squires, T. G. Mason, *Annu. Rev. Fluid Mech.* 42, 413-438, **2010**

[2] A. Mukhopadhyay, S. Granick, *Curr. Opin. Colloid In.* 6, 423-429, **2001**
[3] N. Frickel, R. Messing, A. M. Schmidt, *J. Mater. Chem.* 21, 8466-8474, **2011**

Magneto-mechanical Coupling in Ferrohydrogels

L. Roeder[1], R. Messing[1], P. Bender[2], A. J. Mesko[3], L. Belkoura[1], R. Birringer[2], A. M. Schmidt[1,*]

[1] *Department Chemie, Institut für Physikalische Chemie, Universität zu Köln, Luxemburger Str. 116, D-50939 Köln, *E-Mail: schmidt.annette@uni-koeln.de*
[2] *FB Physik, Gebäude D2$_2$, Universität des Saarlandes, 66041 Saarbrücken*
[3] *University of Tulsa, Tulsa, OK 74104, USA*

Hybrid nanomaterials are obtained by the combination of inorganic and organic compounds to implement different functions and characteristics within a single material. The integration of magnetic nanoparticles into swollen polymer networks, resulting in so-called ferrogels, implies the possibility to combine magnetic and gel-like properties. This way, new magneto-responsive materials are created that are of interest due to the potential opportunities they offer in different practical applications like artificial muscles, actuators or micro-machines.[1]
For the optimization of their unique properties, it is essential to understand the magnetomechanical behavior of the ferrogel composites. We present a novel class of ferrohydrogels involving polyacrylamide (PAAm) segments and ferromagnetic ellipsoid and rod-like particles (Fig. 1).

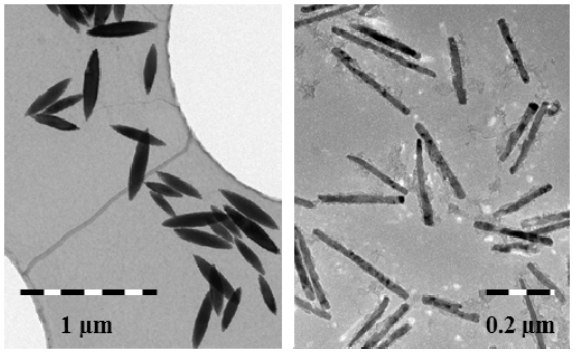

Fig. 1: TEM image of hematite ellipses (left) and nickel rods (right).

For this reason hematite ellipsoids and nickel rods are embedded in PAAm hydrogel matrices of different architecture. In one type of gel, the particles are trapped in the gel matrix by conventional cross-linking (Scheme 1 left), while the particles are not linked chemically to the matrix polymer. The other gel architecture implies particle-linked ferrohydrogels, where the particles serve as multifunctional cross-linkers of the network (Scheme 1 right). Functionalized particles are covalently linked to the polymer segments so that the mechanical response is directly transferred to the polymer network and generates a novel actuation mechanism.[1-3]

Scheme 1: MBA-crosslinked ferrohydrogel with ellipsoids (left) and ellipsoid crosslinked ferrohydrogel (right).

For both architectures, the magnetic behavior of the embedded elongated magnetic nanoparticles is investigated. For this purpose quasi-static magnetometry is used to get information on the mechanical interaction between the particles and the matrix, and provides information on the elastic restoring force.
Our results give insight into the network architecture and the local magnetomechanical behavior of the novel materials. The method may be generalized as an access to nanorheological properties of soft matter by magnetic particle nanorheology.

Acknowledgments

We acknowledge the DFG for financial support in the framework of SPP1259, “Intelligent Hydrogels”.

References

[1] N. Frickel, R. Messing, A. M. Schmidt, *J. Mater. Chem.* (21), 8466-8474, **2011**.
[2] R. Messing, N. Frickel, L. Belkoura, R. Strey, H. Rahn, S. Odenbach, A. M. Schmidt, *Macromol.* (44), 2990-2999, **2011**.
[3] N. Frickel, R. Messing, T. Gelbrich, A. M. Schmidt, *Langmuir* (26), 2839-2846, **2010**.

Estimation of the shear modulus of hydrogels by magneto-optical transmission measurements using ferromagnetic nanorods as local probes

C. Schopphoven, E. Wagner, P. Bender, A. Tschöpe, R. Birringer

Technische Physik, Universität des Saarlandes, 66041 Saarbrücken, Germany

1. Introduction

Nickel nanorods with diameters of 20 nm and aspect ratios of 5-15 nm are ferromagnetic single-domain particles. Due to the uniaxial magnetic shape anisotropy, the magnetic moment is preferentially oriented along the rod axis. When such a nanorod is subjected to a transversal magnetic field, there are in general two processes which contribute to the rotation of the magnetic moment into field direction. First, the magnetic moment rotates out of the anisotropy axis (long rod axis) by an angle Φ (fig.1), working against the anisotropy energy. Second, the entire particle may rotate by an angle ω depending on the mechanical stiffness of the matrix. While the former process reflects the physical properties of the nanorods, the latter is significantly influenced by the properties of the matrix and therefore provides an experimental approach to characterize e.g. the shear modulus of a soft elastic matrix using magnetic nanorods as a probe. In the present study, we employ a combination of magnetic and optical measurements to determine the shear modulus of gelatin-based hydrogels. The magnetic anisotropy of the nanorods is studied by magnetization measurements on textured samples of nanorods embedded in a rigid matrix (high gelatin concentration). The anisotropic polarizability allows to measure the field-dependent rotation angle ω of the nanorods in a soft matrix by optical transmission. From the combination of magnetic and optical measurements, the shear modulus of gelatin-based hydrogels with various gelatin concentrations is calculated.

2. Experimental

In the current study, the nanorods are synthesized by electrodeposition of Nickel into porous alumina-templates. The nanorods are released from the templates by dissolving the alumina layer in an aqueous sodium hydroxide solution, to which polyvinyl-pyrrolidone (PVP) is added as a surfactant. The suspension is washed until a stable colloidal dispersion of magnetic nanorods in water is realized. The nanorods' mean length and diameter are characterized by electron microscopy (TEM, REM).
These fluids are then used to produce gelatin-based ferrogels with gelatin concentrations between 2 and 10 wt.%. Application of a magnetic field prior to and during gelation results in magnetically textured ferrogels.
These samples are magnetically characterized using a vibrating sample magnetometer (VSM) with the specific objective to determine the effective anisotropy constant of the nanorods. The textured nanorod ferrogels are then investigated by optical transmission measurements. The rotation of the nanorods is obtained from the optical extinction of polarized light as a function of the applied field.

3. Results

In an elastic matrix, the magnetic nanorods

rotate under the influence of a transversal magnetic field until the magnetic torque is balanced by a mechanical counter torque. From the torque balance $T_{mech} = T_{mag}$ the relationship

$$\omega = \frac{m_p}{6GV_pC(n)} \cdot \mu_0 H \sin\Phi \qquad (1)$$

can be derived, where m_p is the mean magnetic moment of a single particle, G is the shear modulus of the matrix, V_p is the mean particle volume and $C(n)$ is an aspect ratio-dependent shape factor. Hence, the shear modulus G of the matrix can be determined from the rotation angle ω of the nanorods as function of the magnetic torque $T_{mag} = \mu_0 H \sin\Phi$.

Due to their acicular shape, the electical polarizabilities along the principal axes of Ni nanorods differ significantly. As a result, the extinction of polarized light depends on the orientation of the nanorods with respect to the polarization direction of the incident light. The maximum or minimum extinction is associated with a particle orientation parallel ($0°$) or perpendicular ($90°$) to the polarization direction, respectively. Using these two limiting values as reference, the rotation angle ω of the same nanorods suspended in a soft matrix and subjected to a transversal magnetic field H can be calculated from the transmitted intensity $I(H)$,

$$\omega(H) = \arccos\sqrt{\frac{\log\left(I(H)/I_{0°}\right)}{\log\left(I_{90°}/I_{0°}\right)}}. \qquad (2)$$

The angle Φ between the magnetic moment and the direction of the magnetic field is *a priori* unkown. However, the rotation of the magnetic moment out of the rod axis is determined by the magnetic anistropy constant K_A and the magnetic moment $m_p = V_pM_s$ for a particular sample of nanorods and can be characterized independently by magnetization measurements of textured nanorod ferrogels with a sufficiently high shear modulus so that $\omega \approx 0$. In this case,

$$\frac{m}{m_s} = \cos\Phi = \frac{M_s}{2K_A}\mu_0 H. \qquad (3)$$

This allows to calculate the rotation angle Φ for any combination of $\omega(H)$ and finally to plot ω as a function of the magnetic torque according to eq.1. The analysis for a $2.5\,wt.-\%$ gelatin-based hydrogel is shown in (fig.2) and provides a shear modulus of $G = 640\,Pa$.

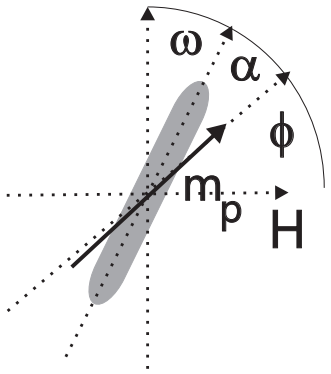

Figure 1: Schematic illustration for the definition of rotation angles.

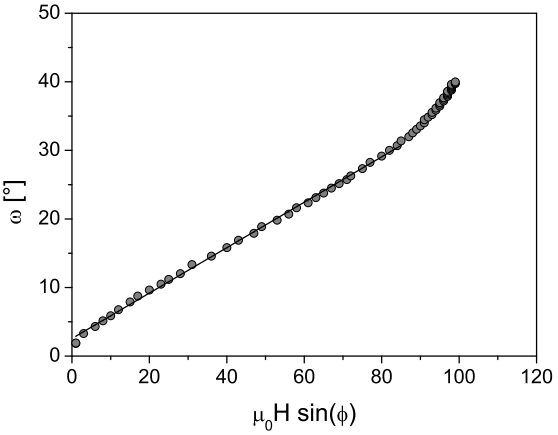

Figure 2: Rotation angle ω as a function of the magnetic torque $T_{mag} = \mu_0 H \sin\Phi$ for a $2.5\,wt. - \%$ gelatin ferrogel using nanorods with $m_p = 4.4 \cdot 10^{-17}\,Am^2$, $V_p = 8.8 \cdot 10^{-23}\,m^3$ and $C(n) = 17.2$. From the slope of a linear fit, a shear modulus of $G = 640\,Pa$ is obtained.

Optically detected hydrodynamic properties of anisotropic magnetic nanoparticles for real time biosensing

S. Schrittwieser[1], J. Schotter[1], A. Schoisengeier[1], K. Soulantica[2], G. Viau[2], L-M. Lacroix[2], S. Lentijo Mozo[2], R. Boubekri[2], F. Ludwig[3], J. Dieckhoff[3], A. Huetten[4], H. Brueckl[1]

[1] *Nano Systems, AIT Austrian Institute of Technology, Vienna, Austria*
[2] *LPCNO (INSA/CNRS/UPS), Toulouse, France*
[3] *Institute of Electrical Measurement and Fundamental Electrical Engineering, TU Braunschweig, Braunschweig, Germany*
[4] *Department of Physics, Bielefeld University, Bielefeld, Germany*

We introduce a novel biosensor concept, which employs hybrid nanoparticles consisting of magnetic nanorods encapsulated by noble metal shells. These nanoparticles have the potential to directly signal the presence of analyte molecules in the sample solution via an increase of the hydrodynamic volume with analyte binding. While the nanoparticles' magnetic cores enable rotation in an external magnetic field, their shells are used to monitor their rotational dynamics through the excitation and observation of longitudinal plasmon resonances (Fig. 1) [1]. We present model calculations on the aspired properties of suitable core-shell nanorods and first experimental results proofing the principle of this measurement method for plain Co-nanorods excited by a rotating magnetic field.

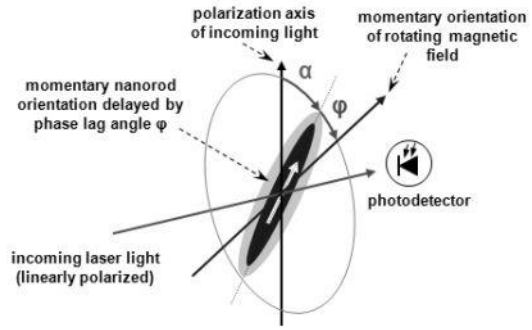

Fig. 1: Concept sketch of nanorod rotation and detection

Method

Our application requires complex multi-component nanoparticles that combine both magnetically and optically anisotropic properties (e.g. an elongated core-shell structure with magnetic core and noble metal shell functionalized by specific antibodies against the target molecule). While we currently strive to realize our aspired hybrid core-shell nanorods, plain Co-nanorods dissolved in organic solutions serve as model system to verify the detection principle (Fig. 2) [2].

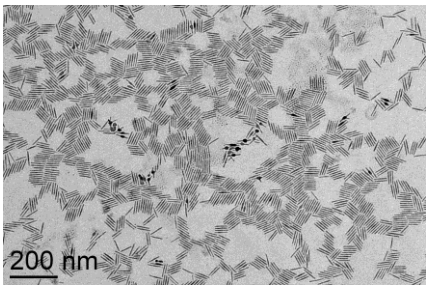

Fig. 2: TEM image of plain Co nanorods (53 nm mean length, 6 nm mean diameter)

We use rotating magnetic fields for alignment control of the nanoparticles in suspension, while their orientation dependent extinction is measured optically (laser diode & photodetector). The phase shift and amplitude of the extinction relative to the rotating field is measured in dependence of field frequency and magnitude as well as nanorod length by a Lock-In amplifier.

Simulation of the optical properties

Discrete dipole approximation calculations [3] of the extinction cross section of a core-

shell nanorod are shown for different angles α of the nanorod's long axis with respect to the polarization axis of the incoming light (see Fig. 3). The resulting longitudinal plasmon peak lies well in the optically transmissive window of serum and whole blood, which opens up the possibility to carry out diagnosis without requiring extensive sample preparation.

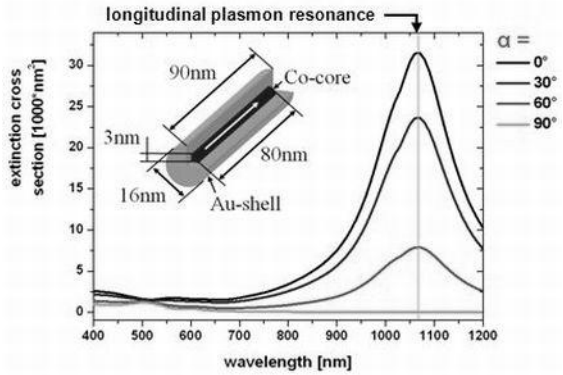

Fig. 3: Modeled variation of the longitudinal plasmon resonance excitation in dependence on the orientation of the rod to the polarization direction of the incident light

Mathematical modeling of rotational behavior

While magnetization processes within solids are well described by the Landau-Lifschitz-Gilbert equation, thermal effects play a major role in ferrofluids. The inclusion of thermal agitation in Gilbert's equation results in the Fokker-Planck equation [4]. Alternatively, Shliomis demonstrated that the dynamics of the magnetization $\vec{M}$ of a small ferrofluid volume under the influence of a magnetic field $\vec{H}$ can be approximated by a simple differential equation which has the following solution for the phase lag angle φ for small angular velocities (ω_H) of an external rotating magnetic field [5]:

$$\varphi = \arctan(\omega_H \tau_{perp}) \qquad (1)$$

Here, τ_{perp} denotes the time constant perpendicular to the magnetic field.

Experimental results

Experimental results demonstrate the evolution of the phase lag of plain Co-nanorods relative to the rotating magnetic field under varying conditions.

Phase measurement results for Co-nanorods in tetrahydrofuran solution with lauric acid serving as surfactant (53 nm mean length and 6 nm diameter) are shown in Fig 4. The expected arctan-behavior as well as saturation at 90° phase lag are confirmed, even though the absolute values still differ from the predicted ones due to particle agglomeration. Measurements on solutions employing different stabilization protocols for obtaining single particle dispersions are currently underway.

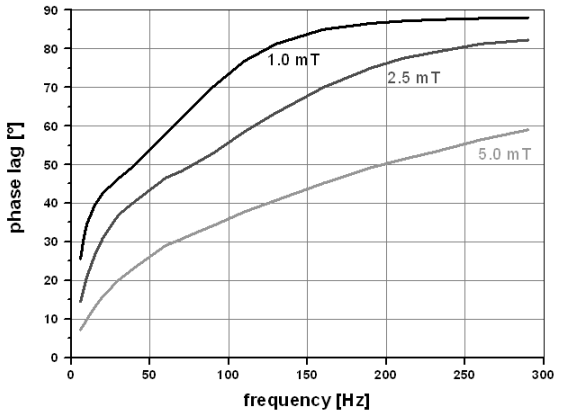

Fig. 4: Phase lag φ of a plain Co-nanorod dispersion for different amplitudes of the rotating magnetic field

Acknowledgments

The research leading to these results has received funding from the European Community's 7th Framework Programme under grant agreement n° NMP4-LA-2010-246479.

References

[1] Schotter et al., Austrian patent number 503845, PCT application number WO/2008/124853.

[2] Wetz et al., Material Science and Engineering C 27 (2007) 1162.

[3] Draine et al., User Guide for the Discrete Dipole Approximation Code DDSCAT 6.1. http://arxiv.org/abs/astro-ph/0409262v2.

[4] Yu et al., Advances in Chemical Physics 87 (1994) 595.

[5] Shliomis, Ferrohydrodynamics: Retrospectives and Issues. In Odenbach S (Ed.), Ferrofluids, Springer-Verlag Berlin Heidelberg 2002.

Thermomagnetic convection in Ferrofluids

L. Sprenger, A. Lange, and S. Odenbach

TU Dresden, Institute of Fluid Mechanics, Chair of Magnetofluiddynamics, 01062 Dresden, Germany

Introduction

Thermomagnetic convection denotes a transport phenomenon in ferrofluids due to a temperature gradient and a magnetic field. Convection sets in when a certain critical Rayleigh number is reached and could be additionally influenced by thermodiffusive processes. Thermodiffusion describes the movement of the fluid's particles in a layer of fluid due to an applied temperature gradient. This phenomenon is also affected by magnetic fields applied to the setup. Recent experimental results [1] motivated further investigations of the correlation of thermomagnetic convection and thermodiffusion.
To fully understand the thermodiffusive effects in ferrofluids the ferrofluid-dynamics theory (FFD) [2] has been developed. From a macroscopic point of view it compiles a rather general partial differential equation (PDE) describing the diffusion driven by gradients of the concentration, temperature, and magnetic field. Besides the numerical solution for this PDE, experiments are to be carried out to validate the numerically obtained data for the Soret coefficient, characterising thermodiffusion.

Experimental Setup

The experiments are carried out with a horizontal layer of fluid and a perpendicular temperature gradient with a cell design based on [3]. The separation process of the fluid is detected by two fluid reservoirs whose change of concentration is determined by sensor coils. The first step to master the process is to evaluate the time-dependent formation of the temperature gradient inside the measuring cell. Figure 1 shows the run of the temperature curve starting by the application of a homogenous middle temperature which is established over the entire cell after about 80 minutes. Then the temperature gradient is applied and it needs about 10 minutes to be present across the cell. The gradient has been observed for three more days and stays constant over the whole time.

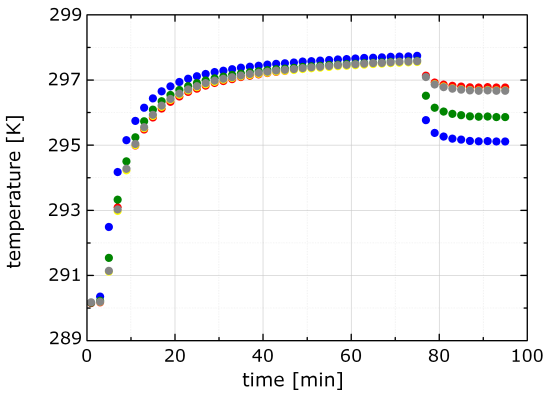

Figure 1: Formation of the temperature gradient in one reservoir starting by the application of a homogenous middle temperature

Detecting the sensor coils' inductivities has been a major challenge so far. Different experimental setups measuring the inductivities reliably with a duration of three days have been tested, but the accuracy had to be questioned. The most promising solution now seems to be detecting the two sensor coils differentially with the help of a bridge circuit whose output voltage stands directly for the concentration gradient over the two reservoirs.

Theoretical Background

The diffusion equation according to [2] is solved in three dimensions numerically with and without the influence of a magnetic field. The solver code used was developed in Gnu Octave using the finite differences method (FDM) to implement the partial derivatives. The time derivative is implemented by the Euler backwards method, the spatial derivatives by central differences.
Figure 2 shows the calculated concentration profile in a non-magnetic setup over the cell height after 20,000 s of separation. By varying the Soret coefficient, the actual influence of the coefficient on the strength of the thermodiffusive separation of the fluid is illustrated. The experimentally expected value is 0.16 1/K [3].
The concentration gradient over the cell is constant at this time regime, the Soret coefficient is thereby part of the inclination of

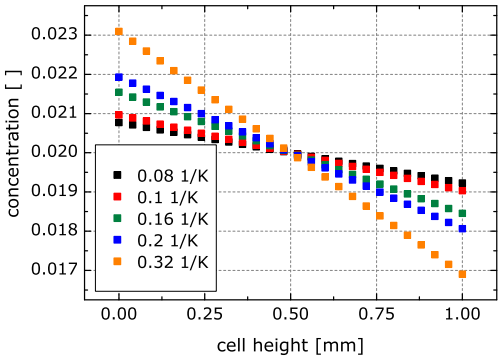

Figure 2: Concentration profiles over the cell height after 20,000 s of separation and varying S_T (without magnetic field)

the curves. In the short time regime, shown in figure 3, concentration profiles with varying Soret coefficients point out that at that time the concentration gradient is not at all constant. The magnetically influenced separation is said to lead to negative Soret coefficients [3] which technically means the opposite movement's direction of the particles. This effect depends on the direction of the temperature gradient and the magnetic field.

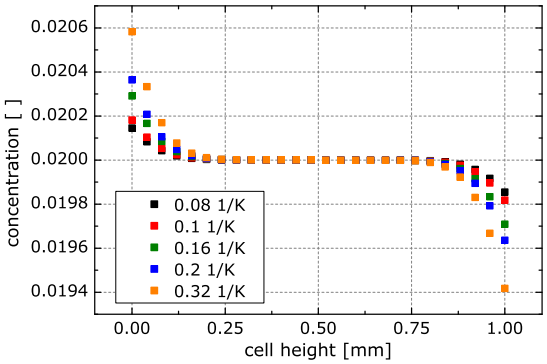

Figure 3: Concentration profiles over the cell height after 200 s of separation and varying S_T (without magnetic field)

Conclusion and Outlook

The determination of the Soret coefficient as well for a non-magnetised as for a magnetised ferrofluid is the main aim of the work. The theoretical work is mostly done and can be used to evaluate the expected experimental data. The reliable knowledge of the dependence of the Soret coefficient on the magnetic field will then be used to describe and investigate the correlation of thermomagnetic convection and thermodiffusion.

Acknowledgments

Financial support by the DFG Grant No. LA 1182/3 is gratefully acknowledged.

References

[1] H. Engler, Diss., Parametrische Modulation thermomagnetischer Konvektion in Ferrofluiden (2010)

[2] A. Lange, Phys. Rev. E **70**, 046308 (2004)

[3] T. Völker, S. Odenbach, Phys. Fluids **17**, 037104 (2005)

Simulation on the anisotropy of the magnetoviscous effect in ferrofluids

Aparna Sreekumari[1], Patrick Ilg[1]
[1] *Polymer Physics, ETH Zürich, Wolfgang-Pauli Str. 10, CH-8093 Zürich*

Motivation

Ferrofluids are stable colloidal suspensions of ferromagnetic nano particles. One of the most important features of ferrofluids is the relative change in viscosity with the change in magnetic field, known as Magneto Viscous Effect (MVE)[1]. Anisotropy of MVE has been proved in a classical experiment by McTague[2]. Shliomis has given a theoretical explanation that the anisotropy of MVE results only from the misalignment of vorticity and magnetic field direction[3]. Zubarev and Iskakova[4] studied the effect of rigid, chain like aggregates on the effective rheological properties of ferrofluids. They predicted that these chain like aggregates give rise to a more complicated anisotropy of the viscosity compared to Shliomis' theory. To get a complete picture of dynamics of ferrofluids, a thorough understanding of the anisotropy of MVE is required. And also, the study of anisotropy is a very sensitive test of ferrofluid theories and it is crucial for modeling ferrofluid flow in practical applications with more complicated geometries.

Plan and Simulation Details

Our aim is to get an improved understanding of the anisotropy of the Magneto Viscous Effect. We study the changes in ferrofluid dynamics, due to the presence of a flow and an applied magnetic field. The typical example of anisotropic fluid is liquid crystals, as in the liquid crystals, we do the same procedure to find the anisotropy by doing different simulations with different orientations of the magnetic field with respect to the flow direction. We do Langevin dynamics of many interacting dipolar particles. We would like to observe magnetisation, structural properties and stresses by following their translational and rotational motion. By comparing the result with experimental work, we hope to get a clear idea about the physical mechanism of observed anisotropy of MVE. Interpretation of the result will be facilitated by the use of magnetite and cobalt based ferrofluids that have been synthesised and carefully characterised in the last years. Careful comparisons with well characterized ferrofluids allow to choose realistic model parameters, with the help of experiments done by Odenbach group[5].

References

[1] S. Odenbach *Magnetoviscous Effects in Ferrofluids*, Lecture Notes in Physics **71**, Springer (2002).

[2] J. P. McTague *Magnetoviscosity of Magnetic Colloids*, The Journal of Chemical Physics **51**, 1, (1969).

[3] M. I. Shliomis, Sov. Phys. JETP **34** (1972) 1291.

[4] A. Yu. Zubarev and L. Yu. Iskakova. Phys. Rev. E **61** (2000) 5415.

[5] M. Gerth-Noritzsch, D. Yu Borin and S. Odenbach, J. Phy. Condens. Matter 2011, in press.

Simulation models for ferrogels

R. Weeber[1], S. Kantorovich[1,2], C. Holm[1]

[1] *Institute for Computational Physics, University of Stuttgart, Pfaffenwladring 27, 70569 Stuttgart, Germany, www.icp.uni-stuttgart.de*
[2] *Ural Federal University, Lenin Av. 51, 620083, Ekaterinburg, Russia, www.usu.ru*

Ferrogels, i.e., hydrogels that additionally contain magnetic single-domain particles, are interesting materials, because their properties arise from an interplay of magnetic and elastic forces. As they can be controlled by tayloring the polymer network forming the gel and by using external magnetic fields to change the interaction of magnetic particles, magnetic gels are considered for applications, e.g., as artificial muscles and drug delivery systems. While many variants of ferrogels can be synthesized today, the detailed microstructure and microdynamics is often unknown.

There are two distinct mechanisms for a ferrogel's change of shape and size under the influence of a homogeneous magnetic field: a deformation can result from the change of the interaction between magnetic particles, as they are aligned by the external field, or it can be caused by the transmission of the torque acting on magnetic particles onto the polymer matrix, which thereby is deformed.

After revisiting two simple 2d computer models which illustrate these two mechanisms, we focus on a 3d model, in which the gel deforms by means of torque transmission. It allows us to have a first glance on magnetic as well as elastic properties. In the model, the gel is built

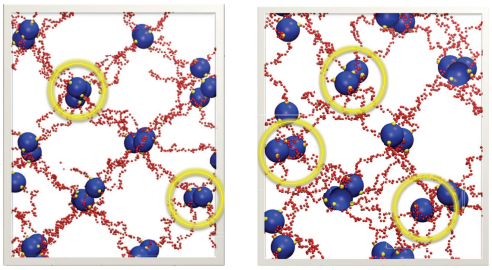

Figure 1: A small part of the gel model without external magnetic field (left), and in a strong field (right). It can be seen that, when a field is applied, the polymer chains are wrapped around the magnetic node particles.

up from 216 magnetic particles forming the nodes of the network. They are initially arranged in a lattice with a cubic unit cell, but are free to move in space during the simulation. Ferroparticles in our model gel are connected with flexible polymer chains which are attached to specific spots on the node particles' surface. Our molecular dynamics simulations show that, when an external magnetic field is applied, the node particles rotate in order to align with the field and, thus, the polymer chains are wrapped around them. This effectively shortens the chains and leads to a shrinking of the gel as a whole. The illustration of this shrinkage is presented in figure 1, where on the left hand side, one can see a simulation snapshot of

the magnetic gel in the absence of a magnetic field. Large particles, here represent magnetic nodes, whereas small particles are the polymer beads. On the right hand side, one finds the snapshot of the ferrogel when the external field is applied. In both pictures, we encircle several magnetic nodes to underline the change in their surrounding. In this way, on the right hand picture, the chains are wrapped around the magnetic nodes.

Acknowledgments

R. Weeber thanks DFG for funding through the SRC Simtech. We are grateful for the financial support of MON s/c 02.740.11.0202, President RF Grant (MK-6415.2010.2) and Alexander von Humboldt foundation.

List of Participants

Christoph Alexiou
Klinik und Poliklinik für Hals-, Nasen- und Ohrenkranke, Waldstr. 1, D- 91054 Erlangen
Tel.: 0049-9131 8534769
Fax: 0049-9131 8534828
E-mail: C.Alexiou@web.de

Franziska Bähring
Universitätsklinikum Jena, Erlanger Allee 101, D-07747 Jena
Tel.: 0049-3641 9325821
Fax: 0049-3641 9325827
E-mail: franziska.baehring@med.uni-jena.de

Silke Behrens
Institut für Katalyseforschung und -technologie, Karlsruher Institut für Technologie, D-76021 Karlsruhe
Tel.: 0049-721 60826512
Fax: 0049-721 60822244
E-mail: silke.behrens@kit.edu

Philipp Bender
Universität des Saarlandes, FR 7.3 Technische Physik / Prof. Dr. Rainer Birringer, Campus D2 2, Postfach 151150
Tel.: 0049-681 3025189
Fax: 0049-681 3025222
E-mail: philipp-bender@web.de

Tünde Borbath
TU Dresden, Institut für Strömungsmechanik, Lehrstuhl Magnetofluiddynamik, D-01062 Dresden
E-mail: borbath.tunde@gmail.com

Dmitry Borin
TU Dresden, Institut für Strömungsmechanik, Lehrstuhl Magnetofluiddynamik, D-01062 Dresden
Tel.: 0049-351 46332307
Fax: 0049-351 46333384
E-mail: dmitry.borin@tu-dresden.de

Alexey Bushmelev
Universität zu Köln, Luxemburger Strasse 116, D-50939 Köln
Tel.: 0049-221 4705472
Fax: 0049-221 4705482
E-mail: alexey.bushmelev@uni-koeln.de

Norbert Buske
MagneticFluids, Köpenicker Landstr. 203, D-12437 Berlin
Tel.: 0049-30 53007805
E-mail: n.buske@magneticfluids.de

Joachim Clement
Universitätsklinikum Jena, Erlanger Allee 101, D-07747 Jena
Tel.: 0049-3641 9325820
Fax: 0049-3641 9325827
E-mail: joachim.clement@med.uni-jena.de

Haimanti Datta
Universität Köln, Department Chemie, D-50939 Köln
Tel.: 0049-221 4705473
E-mail: hdatta@uni-koeln.de

Jan Dieckhoff
TU Braunschweig, EMG, Hans-Sommer-Strasse 66, D-38106 Braunschweig
Tel.: 0049-531 3913876
E-mail: j.dieckhoff@tu-bs.de

Silvio Dutz
IPHT Jena, Albert-Einstein-Straße 9, D-07745 Jena
Tel.: 0049-3641 206319
Fax: 0049-3641 206139
E-mail: silvio.dutz@ipht-jena.de

Dietmar Eberbeck
Physikalisch-Technische Bundesanstalt Berlin, Abbestr. 2-12, D-10587 Berlin
Tel.: 0049-30 34817208
Fax: 0049-30 34817361
E-mail: dietmar.eberbeck@ptb.de

Marc Effertz
Universität Köln, Department Chemie, D-50939 Köln
Tel.: 0049-221 4701871
Fax: 0049-221 4705482
E-mail: effertzm@smail.uni-koeln.de

Sarah Essig
Karlruher Institut für Technologie, Hermann-von-Helmholtz-Platz 1, D-76344 Eggenstein
Tel.: 0049-721 60824320
Fax: 0049-721 60822244
E-mail: sarah.essig@kit.edu

Kurt Gitter
TU Dresden, Institut für Strömungsmechanik, Lehrstuhl Magnetofluiddynamik, D-01062 Dresden
Tel.: 0049-351 46334863
Fax: 0049-351 46333384
E-mail: kurt.gitter@tu-dresden.de

Angelika Gorschinski
KIT, Campus Nord, Hermann-von-Helmholtz-Platz 1, D-76344 Eggenstein
Tel.: 0049-721 60824229
Fax: 0049-721 60822244
E-mail: angelika.gorschinski@kit.edu

Thomas Gundermann
Technische Universität Dresden, Lehrstuhl für Magnetofluiddynamik, D-01062 Dresden
Tel.: 0049-351 46334672
Fax: 0049-351 46333384
E-mail: thomas.grundmann@tu-dresden.de

Dirk Heinrich
TU Berlin, Hardenbergstraße 36, D-10623 Berlin
Tel.: 0049-30 31422476
Fax: 0049-30 31427705
E-mail: dhein@physik.tu-berliln.de

Hongyan Jiang
Universität Köln, Physikalische Chemie, D-50939 Köln
Tel.: 0049-221 4705471
Fax: 0049-221 47050939
E-mail: hjiang@uni-koeln.de

Sofia Kantorovich
Universität Stuttgart, Institute for Computational Physics, Pfaffenwaldring 27, D-70569 Stuttgart
Tel.: 0049-711 68563757
Fax: 0049-711 68563658
E-mail: sofia@icp.uni-stuttgart.de

Klim Kavaliou
Otto-von-Guericke-Universität Magdeburg, IAN, Universitätsplatz 2, D-39106 Magdeburg
E-mail: klim.kavaliou@st.ovgu.de

Martin Krichler
Technische Universität Dresden, Lehrstuhl für Magnetofluiddynamik, D-01062 Dresden
Tel.: 0049-351 46334672
Fax: 0049-351 46333384
E-mail: martin.krichler@tu-dresden.de

Adrian Lange
TU Dresden, Institut für Strömungsmechanik, Lehrstuhl Magnetofluiddynamik, D-01062 Dresden
Tel.: 0049-351 46339867
Fax: 0049-351 46333384
E-mail: adrian.lange@tu-dresden.de

Julia Linke
Technische Universität Dresden, Lehrstuhl für Magnetofluiddynamik, D-01062 Dresden
Tel.: 0049-351 46332068
Fax: 0049-351 46333384
E-mail: julia.linke@tu-dresden.de

Norbert Löwa
Physikalisch-Technische Bundesanstalt, Abbestr. 2-12, D-10587 Berlin
Tel.: 0049-30 34817736
E-mail: norbert.loewa@ptb.de

Peter Löwel
Experimentalphysik 5, Universität Bayreuth, D-95440 Bayreuth
Tel.: 0049-921 553336
Fax: 0049-921 553647
E-mail: s1peloew@stmail.uni-bayreuth.de

Frank Ludwig
Technische Universität Braunschweig, Institut für Elektrische Messtechnik und Grundlagen der Elektrotechnik, Hans-Sommer-Straße 66, D-38106 Braunschweig
Tel.: 0049-531 3913863
Fax: 0049-531 3915768
E-mail: f.ludwig@tu-bs.de

Stefan Lyer
Klinik und Poliklinik für Hals-, Nasen- und Ohrenkranke, Waldstr. 1, D-91054 Erlangen
Tel.: 0049-9131 8534769
Fax: 0049-9131 8534828
E-mail: stefan.lyer@uk-erlangen.de

Gernot Marten
Universität zu Köln, Department Chemie, Luxemburger Strasse 116, D-50939 Köln
Tel.: 0049-221 4705472
Fax: 0049-221 4705482
E-mail: gernot.marten@uni-koeln.de

Florian Johannes Maier
Experimentalphysik 5, Universität Bayreuth, D-95440 Bayreuth
Fax: 0049-921 553647
E-mail: florian.j.maier@stmail.uni-bayreuth.de

Nina Mattoussevitch
STREM Chemicals GmbH, Berliner Str. 56, D-77 694 Kehl
Tel.: (0033) 390-245 222
E-mail: nina-stremgmbh@web.de

Robert Müller
IPHT, Albert-Einstein-Str. 9, D-07745 Jena
E-mail: robert.mueller@ipht-jena.de

Stefan Odenbach
TU Dresden, Institut für Strömungsmechanik, Lehrstuhl Magnetofluiddynamik, D-01062 Dresden
Tel.: 0049-351 46332062
Fax: 0049-351 46333384
E-mail: stefan.odenbach@tu-dresden.de

Simon Pelz
Universität Köln, Department Chemie, D-50939 Köln
Tel.: 0049-221 4704557
Fax: 0049-221 4705482
E-mail: spelz@uni-koeln.de

Harald Pleiner
Max-Planck-Institut für Polymerforschung, Postfach 3148, D-55021 Mainz
Tel.: 0049-6131 379246
Fax: 0049-6131 379340
E-mail: pleiner@mpip-mainz.mpg.de

Jana Popp
Technische Universität Ilmenau, Technische Mechanik, PF 100565, D-98684 Ilmenau
Tel.: 0049-3677 691845
Fax: 0049-3677 691823
E-mail: jana.popp@tu-ilmenau.de

Elena Pyanzina
Ural Federal University, Lenin Av. 51, RU-620083 Ekaterinburg, Russia
Tel.: 007-343 3507541
Fax: 007-343 3507401
E-mail: elena.pyanzina@usu.ru

Helene Rahn
TU Dresden, Institut für Strömungsmechanik, Lehrstuhl Magnetofluiddynamik, D-01062 Dresden
Tel.: 0049-351 4633453
Fax: 0049-351 46333384
E-mail: helene.rahn@tu-dresden.de

Reinhard Richter
Experimentalphysik 5, Universität Bayreuth, D-95440 Bayreuth
Tel.: 0049-921 553351
Fax: 0049-921 553647
E-mail: reinhard.richter@uni-bayreuth.de

Eric Roeben
Universität Köln, Department Chemie, D-50939 Köln
Tel.: 0049-221 4705173
E-mail: eric.roeben@web.de

Lisa Roeder
Universität Köln, Department Chemie, D-50939 Köln
Tel.: 0049-221 4705472
Fax: 0049-221 4705482
E-mail: lisa.roeder@uni-koeln.de

Ekrem Sahin
Institut für Katalyseforschung und -technologie, Karlsruher Institut für Technologie, D-76131 Karlsruhe
Tel.: 0049-721 60822394
E-mail: ekrem.sahin@kit.edu

Annette Schmidt
Universität zu Köln, Luxemburger Strasse 116, D-50939 Köln
Tel.: 0049-221 4705410
Fax: 0049-221 4705482
E-mail: annette.schmidt@uni-koeln.de

Christoph Schopphoven
Universität des Saarlandes, Technische Physik, D-66123 Saarbrücken
Tel.: 0049-681 3025189
E-mail: christoph@schopphoven.de

Joerg Schotter
Austrian Institute of Technology, Donau-City-Straße 1, A-1220 Wien, Austria
Tel.: 0043-50 5504308
Fax: 0043-50 5504399
E-mail: joerg.schotter@ait.ac.at

Stefan Schrittwieser
Austrian Institute of Technology, Donau-City-Straße 1, A-1220 Wien, Austria
Tel.: 0043-50 5504309
Fax: 0043-50 5504399
E-mail: stefan.schrittwieser.fl@ait.ac.at

Silvio Sollazo
Universität Köln, Department Chemie, D-50939 Köln
Tel.: 0221-470 5473
E-mail: sisollazzo@aol.com

Lisa Sprenger
Technische Universität Dresden, Lehrstuhl für Magnetofluiddynamik, D-01062 Dresden
Tel.: 0049-351 46332034
Fax: 0049-351 4633384
E-mail: lisa.sprenger@tu-dresden.de

Aparna Sreekumari
ETH Zürich, Altwiesenstrasse 84, CH-8051 Zürich, Switzerland
Tel.: 0041-44 6336862
E-mail: aparna.sreekumari@mat.ethz.ch

Klaus Stierstadt
Mainzer Str. 16a
80804 München
Tel.: 089- 3689327

Hannah Sustkova
TU Dresden, Institut für Strömungsmechanik, Lehrstuhl Magnetofluiddynamik, D-01062 Dresden
E-mail: LadyEster@seznam.cz

Rainer Tietze
Klinik und Poliklinik für Hals-, Nasen- und Ohrenkranke, Waldstr. 1, D-91054 Erlangen
Tel.: 0049-9131 8534769
Fax: 0049-9131 8534828
E-mail: rainer.tietze@uk-erlangen.de

Andreas Tschöpe
Universität des Saarlandes, Experimentalphysik, D-66123 Saarbrücken
Tel.: 0049-681 3025187
Fax: 0049-681 3025222
E-mail: antsch@mx.uni-saarland.de

Sylvia Türk
TU Dresden, Institut für Strömungsmechanik, Lehrstuhl Magnetofluiddynamik, D-01062 Dresden
Tel.: 0049-351 46334819
Fax: 0049-351 46333384
E-mail: sylvia.tuerk@tu-dresden.de

Rudolf Weeber
Institute for Computational Physics, Universität Stuttgart, Pfaffenwaldring 27, D-70569 Stuttgart
Tel.: 0049-711 68567609
Fax: 0049-711 68563658
E-mail: rudolf.weeber@icp.uni-stuttgart.de